



EXPERIMENTAL FLUTTER ANALYSIS ON AN AIRCRAFT WING



PASUMARTI LEELA NAGA SATYA SUMANTH
18951A2149

EXPERIMENTAL FLUTTER ANALYSIS ON AN AIRCRAFT WING

A Project Report

*Submitted in partial fulfillment of the
Requirements for the award of the degree of*

Bachelor of Technology
In
AERONAUTICAL ENGINEERING

By

P.L.N.S. SUMANTH
18951A2149



DEPARTMENT OF AERONAUTICAL ENGINEERING
INSTITUTE OF AERONAUTICAL ENGINEERING
(Autonomous)
Dundigal, Hyderabad – 500 043, Telangana,
MAY 2022.

DECLARATION

I certify that

- a. The work contained in this report is original and has been done by me under the guidance of my supervisor(s).
- b. The work has not been submitted to any other Institute for any degree or diploma.
- c. I have followed the guidelines provided by the Institute in preparing the report.
- d. I have conformed to the norms and guidelines given in the Ethical Code of Conduct of the Institute.
- e. Whenever I have used materials (data, theoretical analysis, figures, and text) from other sources, I have given due credit to them by citing them in the text of the report and giving their details in the references. Further, I have taken permission from the copyright owners of the sources, whenever necessary.

Place:

Signature of the Student

Date:

Roll No:

APPROVAL SHEET

This project report entitled EXPERIMENTAL FLUTTER ANALYSIS ON AN AIRCRAFT WING by KARTHIKEYA GOUD Y, P.L.N.S. SUMANTH, and A.BHUVANESHWARI is approved for the award of the Degree Bachelor of Technology in AERONAUTICAL ENGINEERING.

Examiner

Supervisor

Principal

Date : _____

Place : _____

ACKNOWLEDGEMENT

We would like to express our respect and indebtedness to all those who gave us the prospect to finish this report successfully. Special thanks are due to our faculty advisor **Mr. R. SABARI VIHAR** whose help, suggestions and encouragement helped us in all time of fabrication process and in writing this report. We also sincerely thank you for the time spent proofreading and correcting our mistakes.

We would love to admit this with much appreciation, the vital role of the Principal **Dr. L V Narasimha Prasad**, Head of the Department **Dr. D Govardhan**, faculty and the staff in AERONAUTICAL DEPARTMENT AND LABORATORY who gave us permission to use the lab equipment and all the necessary tools in the laboratory.

We are also thankful to all our friends who have been always helping us throughout the development of this project with their abilities. Thank you all for your kind cooperation and encouragement which helped us in completion of this project.

ABSTRACT

Flutter is a phenomenon that occurs in structures which are subjected to aerodynamic forces. Vibrations are the oscillations that occur in a structure when disturbed from its original state. As the wing model flies at increasing speeds and increasing angle of attack the vibrations get increased and the frequency of these modes coincide with each other which leads to resonance, this is called **Flutter** and this may lead to catastrophic failures in the aircraft flight. The wing models in this experiment are elastically supported in pitch mode in the test section of the wind tunnel. We assume the wind tunnel test section conditions are the same as the mean sea level conditions. Here for an experimental test, an appropriate wing model design includes various parameters that need to be selected according to the wind-tunnel test conditions. The material used for skin is monokote, spars are made of aluminum, ribs are made of balsa wood. We follow an iterative approach in which angle of attack and true airspeed are constant per iteration.

In the present note, using known computational models, the basic parameters we are going to use are DESIGN LIFT COEFFICIENT and LOCATION OF MAXIMUM CAMBER, the flutter response of the wing models is detected experimentally with the help of accelerometers placed at the forwardmost point of the model (leading edge) and rare most point of the model (trailing edge) of the aeroelastic models. The aeroelastic models we use in the present experiment have two degrees of freedom; thus it has 2 modes of natural vibration, these wing models with accelerometer setup are placed in the test section of the wind tunnel where arduino uno gives the code to encrypt the flutter response to save the values from each iteration; by the observation of this iterative approach we can reach a conclusion. This experimental flutter analysis on aircraft wings ensures that flutter does not occur if we make sure the model strictly operates in its design limitations.

CONTENTS

DECLARATION	iii
APPROVAL SHEET	iv
ACKNOWLEDGEMENT	v
ABSTRACT	vi
CONTENTS	vii
LIST OF FIGURES	viii
1 Introduction	2
2 Review of Relevant Literature	4
3 Methodology	8
Model selection	8
NACA 5 DIGIT SERIES AIRFOIL NOMENCLATURE - “34015”	9
NACA 5 DIGIT SERIES AIRFOIL NOMENCLATURE- “24015”	9
NACA 5 DIGIT SERIES AIRFOIL NOMENCLATURE- “31015”	10
Main parameters	10
Fabrication of the wing models	11
WIND TUNNEL TEST SECTION	12
Coordinate system	12
ARDUINO UNO Setup:	12
EXPERIMENTAL PROCESS	14
4 Results and discussion	18
5 Conclusion and Future scope	49
6 References	51
7 Appendix	53

LIST OF FIGURES

Figure 1.1: Collars triangle.....	2
Figure 3.1:wing model with NACA 31015, NACA 24015 and NACA 34015	9
Figure 3.2: Laser cutting file Figure 3.3: ribs during laser cutting	11
Figure 3.4: Ribs and spars after laser cutting	11
Figure 3.5: low speed wind tunnel.....	12
Figure 3.6: accelerometer adxl 345.....	13
Figure 3.7: aurdino uno board	13
Figure 3.8: aurdino setup with wing mounted in a wind tunnel.....	14
Figure 3.9: NACA 24015, 34015, 31015 mounted in wind tunnel with accelerometer fixed at TE.....	17
Figure 3.10: NACA 34015 mounted in wind tunnel with accelerometer fixed at LE .17	
Figure 4.1: NACA 24015- 00 AOA- ACCELERATION VS TIME at 6.37m/s VELOCITY	19
Figure 4.2: NACA 24015- 00 AOA- ACCELERATION VS FREQUENCY at 6.37m/s VELOCITY.....	19
Figure 4.3: NACA 24015- 00 AOA- ACCELERATION VS TIME at 10m/s VELOCITY.....	20
Figure 4.4: NACA 24015- 00 AOA- ACCELERATION VS FREQUENCY at 10m/s VELOCITY.....	20
Figure 4.5: NACA 24015- 00 AOA- ACCELERATION VS TIME at 13.7m/s VELOCITY.....	21
Figure 4.6: NACA 24015- 00 AOA- ACCELERATION VS FREQUENCY at 13.7m/s VELOCITY.....	21
Figure 4.7: NACA 24015- 00 AOA- ACCELERATION VS TIME AT 17.4 m/s VELOCITY.....	22
Figure 4.8: NACA 24015- 00 AOA- ACCELERATION VS TIME & FREQUENCY AT 17.4 m/s VELOCITY	22
Figure 4.9: NACA 24015- 00 AOA- ACCELERATION VS TIME AT 21.2 m/s VELOCITY.....	23

Figure 4.10: NACA 24015- 00 AOA- ACCELERATION VS FREQUENCY AT 21.2 m/s VELOCITY	23
Figure 4.11: NACA 24015- 00 AOA- ACCELERATION VS TIME AT 25.1 m/s VELOCITY.....	24
Figure 4.12: NACA 24015- 00 AOA- ACCELERATION VS FREQUENCY AT 25.1 m/s VELOCITY	24
Figure 4.13: NACA 24015- 00 AOA- ACCELERATION VS FREQUENCY & TIME AT 28.8 m/s VELOCITY	25
Figure 4.14: NACA 24015- 00 AOA- ACCELERATION VS FREQUENCY AT ...	25
Figure 4.15: NACA 24015- 00 AOA- ACCELERATION VS TIME AT 32.7 m/s VELOCITY.....	26
Figure 4.16: NACA 24015- 00 AOA- ACCELERATION VS FREQUENCY AT 32.7 m/s VELOCITY	26
Figure 4.17: NACA 24015- 50 AOA- ACCELERATION VS TIME.....	27
Figure 4.18: NACA 24015- 50 AOA- ACCELERATION VS FREQUENCY AT ...	27
Figure 4.19: NACA 24015- 50 AOA- ACCELERATION VS TIME AT 10 m/s VELOCITY.....	28
Figure 4.20: NACA 24015- 50 AOA- ACCELERATION VS FREQUENCY AT 10 m/s VELOCITY	28
Figure 4.21: NACA 24015- 50 AOA- ACCELERATION VS TIME AT 13.7 m/s VELOCITY.....	29
Figure 4.22: NACA 24015- 50 AOA- ACCELERATION VS FREQUENCY AT 13.7 m/s VELOCITY	29
Figure 4.23: NACA 24015- 50 AOA- ACCELERATION VS TIME AT 17.4 m/s VELOCITY.....	30
Figure 4.24: NACA 24015- 50 AOA- ACCELERATION VS FREQUENCY AT 17.4 m/s VELOCITY	30
Figure 4.25: NACA 24015- 50 AOA- ACCELERATION VS TIME AT 21.2 m/s VELOCITY.....	31
Figure 4.26: NACA 24015- 50 AOA- ACCELERATION VS FREQUENCY AT 21.2 m/s VELOCITY	31
Figure 4.27: NACA 24015- 50 AOA- ACCELERATION VS TIME AT 25.1 m/s VELOCITY.....	32

Figure 4.28: NACA 24015- 50 AOA- ACCELERATION VS FREQUENCY AT 25.1 m/s VELOCITY	32
Figure 4.29: NACA 24015- 50 AOA- ACCELERATION VS TIME AT 28.8m/s VELOCITY.....	33
Figure 4.30: NACA 24015- 50 AOA- ACCELERATION VS FREQUENCY AT 28.8 m/s VELOCITY	33
Figure 4.31: NACA 24015- 100 AOA- ACCELERATION VS TIME AT 6.37 m/s VELOCITY.....	34
Figure 4.32: NACA 24015- 100 AOA- ACCELERATION VS FREQUENCY AT 6.37 m/s VELOCITY.....	34
Figure 4.33: NACA 24015- 100 AOA- ACCELERATION VS FREQUENCY AT 10 m/s VELOCITY	35
Figure 4.34: NACA 24015- 100 AOA- ACCELERATION VS TIME AT 10 m/s VELOCITY.....	35
Figure 4.35: NACA 24015- 100 AOA- ACCELERATION VS TIME AT 13.7 m/s VELOCITY.....	36
Figure 4.36: NACA 24015- 100 AOA- ACCELERATION VS FREQUENCY AT 13.7 m/s VELOCITY.....	36
Figure 4.37: NACA 24015- 100 AOA- ACCELERATION VS TIME AT 17.4 m/s VELOCITY.....	37
Figure 4.38: NACA 24015- 100 AOA- ACCELERATION VS FREQUENCY AT 17.4 m/s VELOCITY.....	37
Figure 4.39: NACA 24015- 100 AOA- ACCELERATION VS TIME AT 21.2 m/s VELOCITY.....	38
Figure 4.40: NACA 24015- 100 AOA- ACCELERATION VS FREQUENCY AT 21.2 m/s VELOCITY.....	38
Figure 4.41: NACA 24015- 100 AOA- ACCELERATION VS TIME AT 25.1m/s VELOCITY.....	39
Figure 4.42: NACA 24015- 100 AOA- ACCELERATION VS FREQUENCY AT 25.1m/s VELOCITY.....	39
Figure 4.43: NACA 24015- 100 AOA- ACCELERATION VS TIME AT 28.8m/s VELOCITY.....	40
Figure 4.44: NACA 24015- 100 AOA- ACCELERATION VS FREQUENCY AT 28.8m/s VELOCITY.....	40

Figure 4.45: NACA 24015- 150 AOA- ACCELERATION VS TIME AT 6.37 m/s VELOCITY.....	41
Figure 4.46: NACA 24015- 150 AOA- ACCELERATION VS FREQUENCY AT 6.37 m/s VELOCITY.....	41
Figure 4.47: NACA 24015- 150 AOA- ACCELERATION VS TIME AT 10 m/s VELOCITY.....	42
Figure 4.48: NACA 24015- 150 AOA- ACCELERATION VS FREQUENCY AT 10 m/s VELOCITY	42
Figure 4.49: NACA 24015- 150 AOA- ACCELERATION VS TIME AT 13.7 m/s VELOCITY.....	43
Figure 4.50: NACA 24015- 150 AOA- ACCELERATION VS FREQUENCY AT 13.7 m/s VELOCITY	43
Figure 4.51: NACA 24015- 150 AOA- ACCELERATION VS TIME AT 17.4 m/s VELOCITY.....	44
Figure 4.52: NACA 24015- 150 AOA- ACCELERATION VS FREQUENCY AT 17.4 m/s VELOCITY	44
Figure 4.53: NACA 24015- 150 AOA- ACCELERATION VS TIME AT 21.2 m/s VELOCITY.....	45
Figure 4.54: NACA 24015- 150 AOA- ACCELERATION VS FREQUENCY AT 21.2 m/s VELOCITY	45
Figure 4.55: NACA 24015- 150 AOA- ACCELERATION VS TIME AT 25.1 m/s VELOCITY.....	46
Figure 4.56: NACA 24015- 150 AOA- ACCELERATION VS FREQUENCY AT 25.1 m/s VELOCITY.....	46
Figure 4.57: NACA 24015- 150 AOA- ACCELERATION VS TIME AT 28.8 m/s VELOCITY.....	47
Figure 4.58: NACA 24015- 150 AOA- ACCELERATION VS FREQUENCY AT 28.8 m/s VELOCITY	47
Figure 4.59: NACA 24015- 150 AOA- ACCELERATION VS TIME AT 32.7 m/s VELOCITY.....	48
Figure 4.60: NACA 24015- 150 AOA- ACCELERATION VS FREQUENCY AT 32.7 m/s VELOCITY	48

LIST OF ABBREVIATIONS

LE - Leading Edge

TE - Trailing Edge

NACA - National Advisory Committee for Aeronautics

C_l - Coefficient Of Lift

Chapter 1

1 Introduction

Aero elasticity is the phenomenon where we study the interaction between the deformations of elastic structure and the resultant aerodynamic forces. Engineers in today's world want to build flying vehicles that are faster and use less fuel, which puts them under pressure to design lifting surfaces that are thinner, lighter, and more flexible. Aero elasticity is therefore important in the design of aircraft lifting surfaces. The deformation of an elastic body in a cross flow due to aerodynamic loads is the focus of aero elasticity. Basic knowledge of dynamics, aerodynamics, and elasticity can be used to investigate two or more interaction phenomena. [20.]

Structural dynamics, static aeroelasticity, and dynamic aero elasticity are only a few examples of interactions. In aero elasticity, the loads (i.e., aerodynamics) are mostly determined by deformation, and the deformation (i.e., structural dynamics) is primarily determined by the loads, resulting in a linked problem. The main area of interest in static aeroelasticity is static instability, also known as "Divergence," while the most important phenomenon in dynamic aero elasticity is Flutter. At threshold airspeed, known as the flutter speed, the self-sustaining motion is shown by aircraft.

Oscillation varies above this speed, producing intense vibrations which can cause structural damage by rising amplitudes or may cause eventual destruction to the aircraft.

In the cross flow; flutter is one of the most extreme forms of instability that an aircraft's wing and tail can show. Both input and output vibration properties of a system are studied to help identify the system on the basis of mass, stiffness, and damping. The measurement of a structure's or machine's natural frequencies is useful in determining the operational speeds of nearby machinery to avoid resonant conditions. [20.]

The literature provides a brief description of the test protocols, equipment, and experimental approach. Different models and experimental setups were used in the experiment, such as the NACA31015, NACA34015, NACA24015 airfoils as well as the wind tunnel setup.

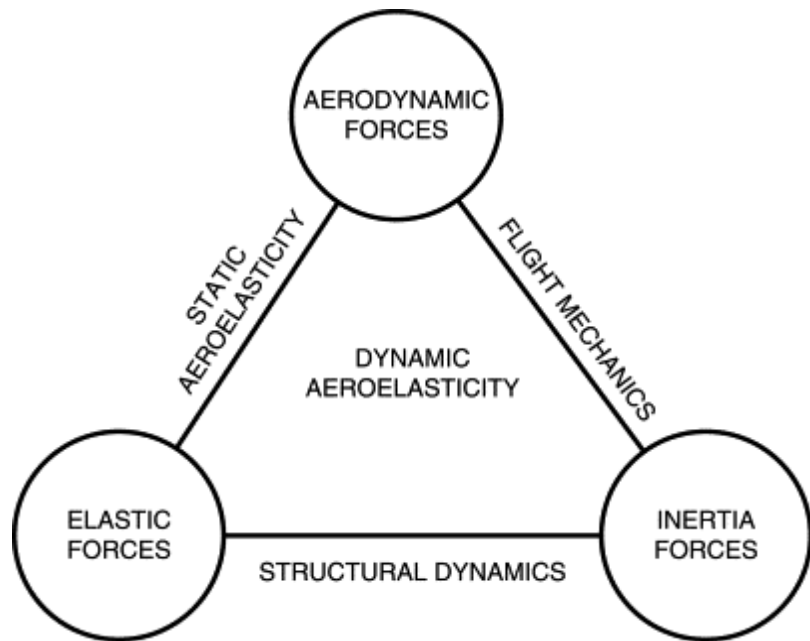


Figure 1.1.1: Collars triangle

Coupling high-level computational fluid dynamic (CFD) methodologies with structural dynamic tools to perform aero elastic analysis is referred to as computational aeroelasticity (CAE). CAE has acquired popularity since significant development has been achieved in CFD, computational structural dynamics (CSD), and computer technology. While computational approaches for studying various elements of aero elastic response have been explored for some time, there are still several unresolved research challenges. Many techniques in computational

aeroelasticity, for example, strive to combine distinct computational methodologies for the aerodynamic and structural dynamic subsystems.[21.]

Flutter, as we recollect, is one of the physical occurrences that tends to happen when a solid's elastic nature/behavior interconnects with the gas or fluid which is naturally passing over it. Flutter is an instability which happens due to the elasticity of the body and varies over a particular time characterized by strong solid-structure vibrations of quickly rising amplitude. It frequently results in either major structural damage or total demolition of the structure.

When the parameters detailing fluid-structure interaction approach's critical values, flutter happens. The physical explanation for this phenomena is that, under certain conditions, the energy of the flow is rapidly absorbed by the structure and converted into mechanical vibration energy. Flutter must be prevented in engineering practice by either designing the structure or implementing a control system capable of suppressing unwanted vibrations. [22.]

Chapter 2

2 Review of Relevant Literature

The prior work should have been thoroughly examined in order to obtain a clear understanding of how to set up an experimental setup for inspection of the flutter response to the changes happening in the test section (as we are following an iterative method of inspection). Flutter analysis has become one of the vital responses. Moreover this is a natural oscillation happening in the bodies of any structure in every human's working area. In this case it is aerospace in recent years, when it was previously designated for airplanes, autos, and other related fields... In 1899, the Wright brothers carried out the first experimental work of aero elasticity. Later, NASA conducted numerous experiments on flutter analysis. The Structural Dynamics Division at NASA Langley Research Center, known as the Benchmark models Program, organized wind tunnel tests to reach their objective. The wing used in the test has the airfoil of NACA 0012 rectangular in shape when seen from top was fixed on the flexible two DOF mount system. There's no inertial connection in between two modes (Pitch/Plunge) because the system was developed that way.[1.]

The pitch and plunge motion parameters were determined using servo accelerometers. The research concentrated on conventional flutter, Stall flutter and plunge instability. Static ports arranged chord wise just on the wing were used to

calculate pressure distributions. As per the findings, the traditional flutter boundary is distinguished by an unusual pattern of increasing dynamic pressure with increasing Mach number. A plunge instability domain was observed in the transonic regime, indicating that plunge mode caused flutter in that regime.[2.]

Later, NASA conducted the research using the same benchmark model but with alternative airfoil wings. Where they tested airfoils named NACA 0012, NACA 64A010, and NACA SC (2)-0414. Classical flutter, transonic stall flutter, and plunge instability were all taken into account this time. The supercritical airfoil was the focus of most experiments. For measuring forces, the experimental setup was not up to the mark and unproven. Dynamic movements were monitored using strain gauges and accelerometers installed on the model. For the data collecting system, benchmark active control technology was employed. Pressure transducers were carefully installed on wing models in a chord wise orientation at a certain span point.[3.]

Chung presented an incremental technique for solving aero elastic issues with free play. Using the NASTRAN software and research has been done regarding data (mode shapes, natural frequencies, and damping) collected from ground vibration measurements, Pankaj developed a system for estimating the flutter characteristics of an aircraft construction. Hasheminejad used the Runge–Kutta technique to compute the open-loop supersonic aero elastic behavior and flutter motion of a rectangular shaped and sandwich plate that has been elastically supported. [4.]

The experimental model was created to test the flutter response and stall flutter properties of the wing in the wind tunnel at the University Of Liege, Belgium. Instead of rods, linear springs were used to describe the pitch and plunge stiffness of the wing in this experimental model. The tests were carried out on NACA 0018's wing's Pitch and plunge motion were measured using accelerometers. Oscillations in the high and low limit cycles were noticed and the real instantaneous velocity on a single plane parallel to the free stream velocity was visualized. Experiments revealed sharp-leading-edge stall flutter behavior caused by vortex shedding and the formation of a laminar separation bubble at the leading edge.[5.]

Bendiksen and Saber investigate fluid–structure interaction problems that involve both structural and fluid nonlinearities. The exploration of nonlinear aero elastic stability constraints with wings with a high aspect ratio. Large deflections cause either aerodynamic and structural nonlinearities, which their finite element

models account for. Svacek proposed a numerical simulation model of two-dimensional incompressible viscous flow coupling with a vibrating airfoil.[6.]

In the pitching direction, Zhen and Yang designed two-dimensional wings with cubic stiffness. The system's flutter velocity was then tested to Hopf bifurcation theory. The unpredictable reactions of an aero elastic system were estimated using a numerical integration method. Pang and Jinglong¹⁸ analyzed the effect of wingtip devices on wing flutter using numerical models. Structural vibration has been determined by a computational structural dynamics (CSDs) solver only with geometric nonlinearity shown in the modeling, and unsteady aerodynamics were simulated using a computational fluid dynamics (CFDs) solver with the Euler equations presented as fluid governing equations.[7.]

The interaction of CFD and CSD is examined, and the limit cycle oscillation response of a basic transport wing is estimated. By utilizing analytical and semi-analytical techniques, researchers have been attempting to forecast the frequency and amplitude of an airfoil's flutter oscillations for many years. The characterizing function approach, also known as harmonic balancing or linearization, is a common way for producing an analogous linear system that can subsequently be evaluated using classic linear aero elastic techniques. Chung proposed an incremental method and used it to solve free-play aero elastic problems. Haul and Chen investigated flutter using ANSYS software and the full-order and multimode methods.[8.]

Kargarnovin and Mamandi explored the effects of a sharp edged gust on an airfoil's reaction and flutter. Wang and Qiu¹¹ investigated the sensitivity of wing flutter speed to structural parameter uncertainty. An interval finite element model was developed and utilized to forecast the flutter critical wind speed range prediction. Bendiksen and Seber research fluid–structure interaction involves both structural and fluid nonlinearities. They looked at nonlinear aero elastic stability issues with high aspect ratio wings. Their finite element models account for both aerodynamic and structural nonlinearities caused by significant deflections. Svacek created a numerical simulation model of the interaction of two-dimensional incompressible viscous flow with a vibrating airfoil.[9]

Aero elastic investigations of airfoil wings have been a fascinating component of the present study topic. Mazidi and Fazelzadeh recently showed the significance of wing sweep angle on the flutter limits of a wing/engine arrangement. A wing with an external storage has also been the subject of several

studies as a common airplane layout. However, there is a scarcity of experimental research on these topics. Dowell and his research group have completed several tests on flutter experiments of a constant thickness cantilever delta wing with external storage. The air speed and flutter velocity are quite modest in the majority of these trials.[10.]

Theodorsen was the first to discover the flutter phenomena in 1935. Since then, a large number of theoretical and experimental researches on this topic have been published, including Ashley and Landahl, Bisplinghoff, and Ashley and Dowell. The desire for fast and nimble aircraft has surged recently. Active flutter suppression strategies are utilized to minimize flutter at low speeds and boost utter crucial speeds. To reduce flutter, Marretta and Marino presented a control flow based on a single input-single output controller. Lee investigated flutter as well as the open and closed-loop responses of a wing flap system employing sliding mode control.[11.]

In low subsonic flow, Dardel and Bakhtiari-Nejad proposed and included a static output feedback control for aero elastic management of a cantilevered rectangular wing. In a lightweight and low aspect ratio rectangle shaped nonlinear structural wing, they developed a control to extend the flutter boundary and suppress limit cycle oscillation. Analytical and semi-analytical methodologies have been used to predict the frequency and amplitude of flutter oscillations through an airfoil for many years. [12.]

This paper focuses on the creation of a numerical tool for aircraft wing fluid-structure interaction (FSI) calculations, in which the exterior airflow and interior structure interact, as well as wind tunnel testing of two half wing prototypes to effectively evaluate the numerical tool's accuracy. For the aerodynamic study, a panel approach was used, and for the structural analysis, a finite-element model with equivalent beam elements was used, both written in the MATLAB programming language. Area, airfoil cross-section shape, aspect ratio, taper ratio, sweep angle, and dihedral angle were used to parameterize the wing design.[19.]

CHAPTER 3

3 Methodology

Model selection

This report offers a comprehensive experimental investigation to identify the flutter phenomenon of the aircraft wing. The experimental setup for determining the flutter response was built for this purpose. The mechanical design is a two-degree-of-freedom system. This arrangement will be capable of analyzing the flutter behavior of any sort of two-dimensional wing. Here in this case wing models with rectangular planform with NACA 34015, NACA 31015, NACA 24015 airfoils are being examined for the wing's flutter response. A rectangular planform is considered because our main aim of experiment is to know the effect of **design lift coefficient and location of maximum camber** on wing flutter.



Figure 3.1: wing model with NACA 31015, NACA 24015 and NACA 34015

NACA 5 DIGIT SERIES AIRFOIL NOMENCLATURE - “34015”

- ‘3’ represents design lift coefficient when multiplied by ‘0.15’(i.e $C_l = 0.45$)
- ‘40’ represents location of maximum camber when divided by ‘2’ (i.e 20% of the chord.)
- ‘15’ represents the maximum thickness of the airfoil. (i.e 15% of the chord.)

NACA 5 DIGIT SERIES AIRFOIL NOMENCLATURE- “24015”

- ‘2’ represents design lift coefficient when multiplied by ‘0.15’ (i.e $C_l = 0.3$)
- ‘40’ represents location of maximum camber when divided by ‘2’ (i.e 20% of the chord)
- ‘15’ represents the maximum thickness of the airfoil.

(i.e 15% of the chord)

NACA 5 DIGIT SERIES AIRFOIL NOMENCLATURE- “31015”

- ‘3’ represents design lift coefficient when multiplied by ‘0.15’(i.e $C_l = 0.45$)
- ‘10’ represents location of maximum camber when divided by ‘2’ (i.e 5% of the chord)
- ‘15’ represents the maximum thickness of the airfoil.
(i.e 15% of the chord)

Main parameters

- design lift coefficient : The camber line of the airfoil is determined by the design lift coefficient. When the design lift coefficient is reached, the flow reaches the airfoil exactly parallel to the start of the camber line. In a simple way we can say the lift coefficient of an airfoil at ‘0’ degree angle of attack is the airfoils design lift coefficient.

This equates to a lift coefficient of $0.15 \times 2 = 0.3$ for a NACA 23015.

- location of maximum camber : Maximum camber is the maximum distance between the mean camber line and the chord line; maximum thickness is the maximum distance between the lower and upper surfaces.

Fabrication of the wing models

- To begin the construction process, we must first create a design layout by printing the design on paper and then assembling the parts.
- The wing's chord length is 240mm, half wingspan (length of half wing from root chord to tip chord) is 450mm and aspect ratio is 1.875.
- We prepared the laser cutting files to make 4 ribs for the wing models and then used a laser cutting tool to cut them out. The material used to make these ribs is 8mm thick balsa wood.
- Wings are the largest portion of an aircraft; so we employ 6mm thick aluminum rods as spars that go into the wings and reinforce the structure.
- Monokote is used as the skin of these wing models which makes the surface of these models lighter and smoother.

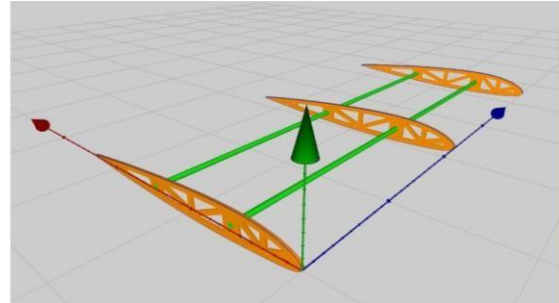


Figure 3.2: Laser cutting file



Figure 3.3: ribs during laser cutting



Figure 3.4: Ribs and spars after laser cutting

WIND TUNNEL TEST SECTION

Coordinate system

- The x-axis is positive in the opposite direction of flow on the model.
- The y-axis is positive in the starboard side of the model in the wind tunnel test section.
- The z-axis is positive in the vertically upward direction of the model.



Figure 3.5: low speed wind tunnel

ARDUINO UNO Setup:

→ Accelerometer

In this experiment we used the ADXL345 accelerometer sensor. It is a package of 3-axis acceleration measurement systems all in a single piece. It has a measurement range of $\pm 16g$ minimum. The ADXL345 uses a single structure for sensing the X,Y and Z axis.

→ Coordinate system

- The x-axis of the accelerometer is positive in the opposite direction of flow on the accelerometer.
- The y-axis is positive in the starboard side of the accelerometer which is attached to the wing model and placed in the wind tunnel test section.
- The z-axis is positive in the vertically upward direction of the accelerometer.

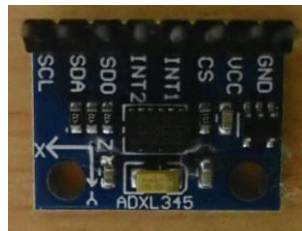


Figure 3.6: accelerometer adxl 345

→ Arduino uno

- Arduino uno board is the device used to transmit the code to the accelerometer where the device helps the sensor to obtain the acceleration in the x,y and z plane along with timestamp.

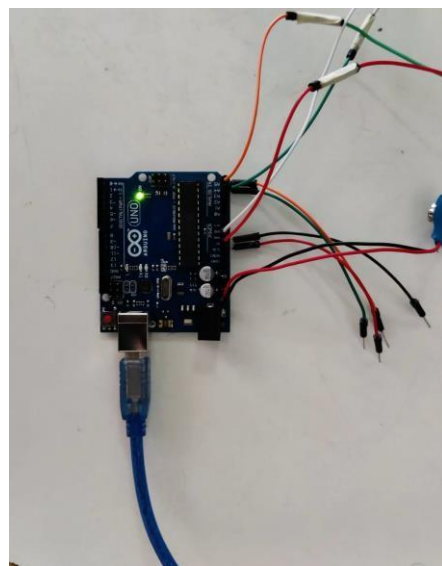


Figure 3.7: aurdino uno board



Figure 3.8: aurdino setup with wing mounted in a wind tunnel

EXPERIMENTAL PROCESS

- The wings with different design lift coefficients are mounted in the wind tunnel at different angles of attack and velocities.
- The constant velocities are obtained from the rpm of the wind tunnel where we can directly change the values of rpm to velocity.
- We can observe the different wings mounted in the wind tunnel with 0 degrees, 5 degrees and 15 degrees of angle of attack with sensors fixed at leading and trailing edges.
- We know that

$$V_{\text{test section}} = \frac{\sqrt{(\rho l \times g \times h \times 2) \div \rho_{\text{air}}}}{\sqrt{1 - \frac{A^2_{\text{test section}}}{A^2_{\text{inlet}}}}}$$

$$\rho_l = 800 \text{ kg/m}^3 \text{ (methyl alcohol)}$$

$$g = 9.81 \text{ m/s}^2 \text{ (approximate)}$$

$$\rho_{\text{air}} = 1.2 \text{ kg/m}^3 \text{ (approximate)}$$

$$v(m / s) = 3.68\sqrt{h(mm)}$$

- By using this formula we convert RPM into velocity.

Table 3.1: The wind tunnel performance readings

RPM	Velocity in the test section(m/s)
0	0
100	3.68
200	6.37
300	10.0
400	13.7
500	17.4
600	21.2
700	25.1
800	28.8
900	32.7
1000	36.3
1100	40.05
1200	43.7
1300	47.2
1400	50.8

- The wings are connected with an accelerometer and arduino where the arduino board transmits the code to an accelerometer through which we get the acceleration variations at certain timestamp values.
- Software required to analyze the values obtained by an accelerometer is MATLAB. We in this experiment used MATLAB R2021A software to perform the analysis.
- The code we have done for this experiment will first read the comma separated value files and import the data of the accelerometer given as the input.
- This input consists of acceleration values in x, y and z direction and the time in seconds. The code will now assign the variables to accelerations in x, y, z directions and time(t).
- These obtained values from the accelerometer are used to convert timestamp values into frequency using FAST FOURIER TRANSFORMS code in MATLAB as mentioned in the following steps.
- In the next step of the code the number of time steps, the sampling time period (time interval per time step) is created.
- Conversion of sampling time period to sampling frequency is performed such that **fs** return the number of intervals not the frequency value, so here the code helps us convert the '**fs**' value to frequency value using '**DFT**' (Discrete Fourier Transform) relations.
- Conversion process of acceleration values from time domain to frequency domain is executed using a fast fourier transform.
- For plotting the Acceleration vs Frequency graph for the LE/TE mounted accelerometer data we gave the axis labels, limit values for Y Axis and then assigned the legend command to plot for LE and TE curves in a single graph.
- Then we generate plots/graphs of velocity versus frequency in MATLAB to compare the results of each and every airfoil to compare and conclude that if there is flutter to that particular design lift coefficient and airfoils.
- Here we compare velocity versus frequency graphs of each airfoil with different design lift coefficients at 0, 5, 10, 15 degrees of angles of attack and at different velocities.

- The results of the flutter are obtained in the form of graphs (i.e v-f graphs), here we can observe the variation in the amplitude of the graphs where the frequency varies so we can conclude the results by looking at the graphs in the results and discussion section.

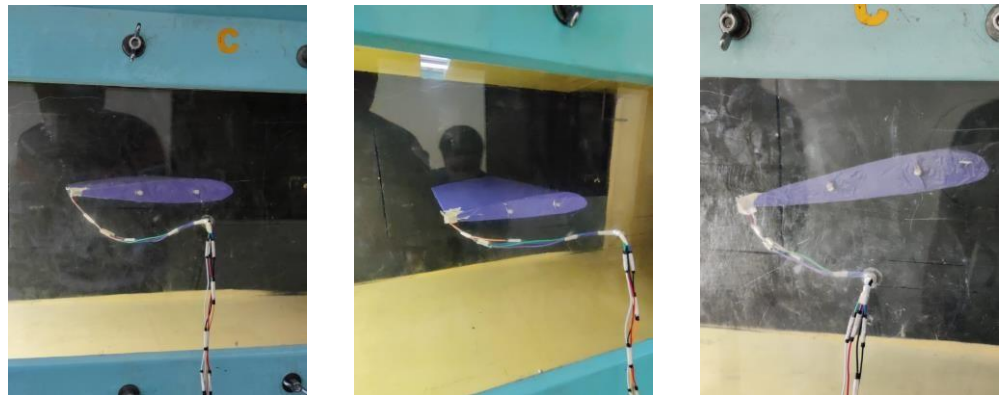


Figure 3.9: NACA 24015, 34015, 31015 mounted in wind tunnel with accelerometer fixed at TE



Figure 3.10: NACA 34015 mounted in wind tunnel with accelerometer fixed at LE

Chapter 4

4 Results and discussion

- Here are the plots which were obtained from the **MATLAB R2021A** software
- These plots were generated for acceleration magnitude vs frequency and also for acceleration vs time graphs.
- Graphs were generated for different wings with variations/change in parameters like Airfoil, Angle of attack, velocities.
- For this experimental flutter analysis on the wing we followed the iterative approach in which we placed our model in the test section and tested the behavior of the model per each inlet velocity per an angle of attack simultaneously.
- Here in the present report we have given the plots of **acceleration amplitude vs time** and **acceleration amplitude vs frequency** of a model which consists of the airfoil named NACA 24015. There are a total of almost 90 iterations performed in the wind tunnel test section including all 3 airfoils whereas we are presenting only 30 of the 90 iterations executed due to the space constraint. (i.e graphs of only NACA 24015)
- results obtained are shown as below graphs:

Iteration 1

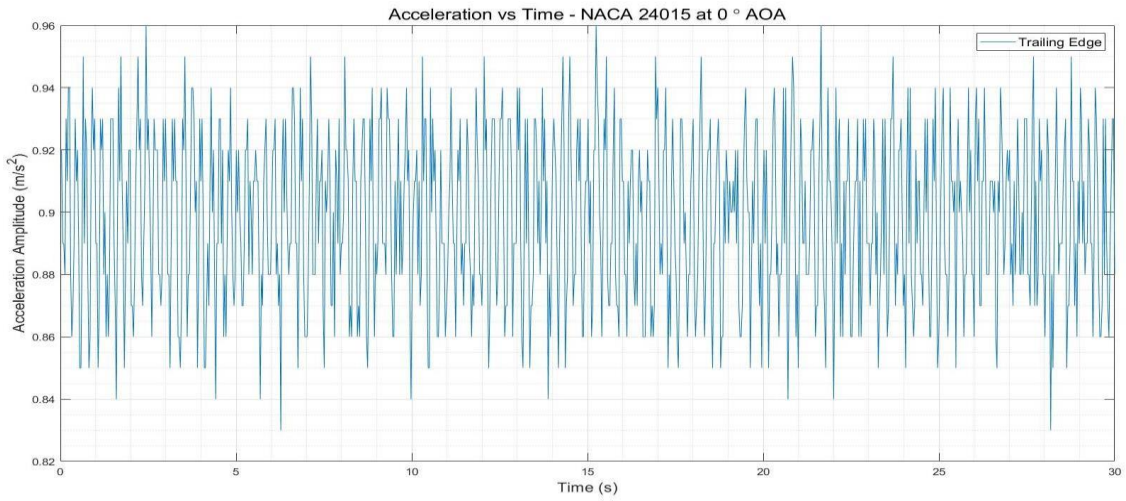


Figure 4.1: NACA 24015- 00 AOA- ACCELERATION VS TIME at 6.37m/s VELOCITY

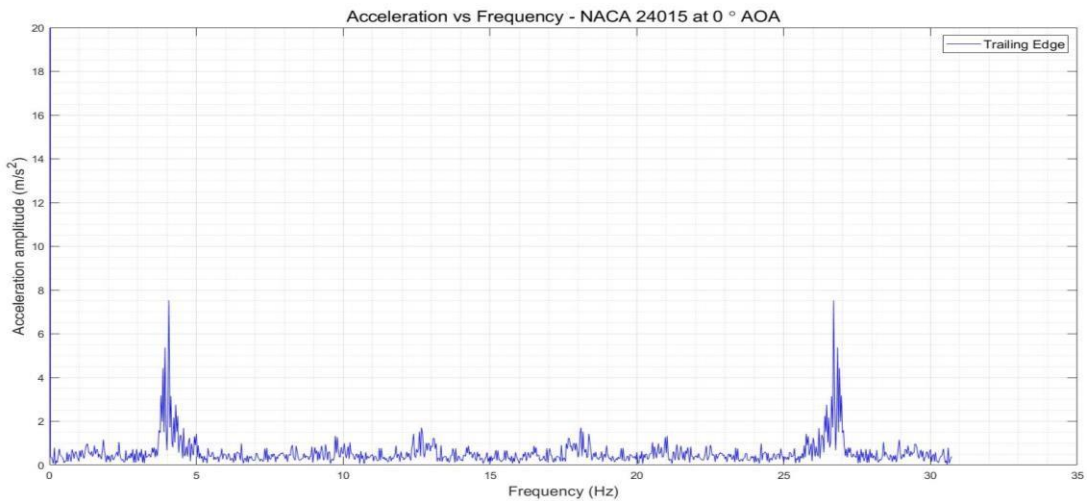


Figure 4.2: NACA 24015- 00 AOA- ACCELERATION VS FREQUENCY at 6.37m/s VELOCITY

Iteration 2

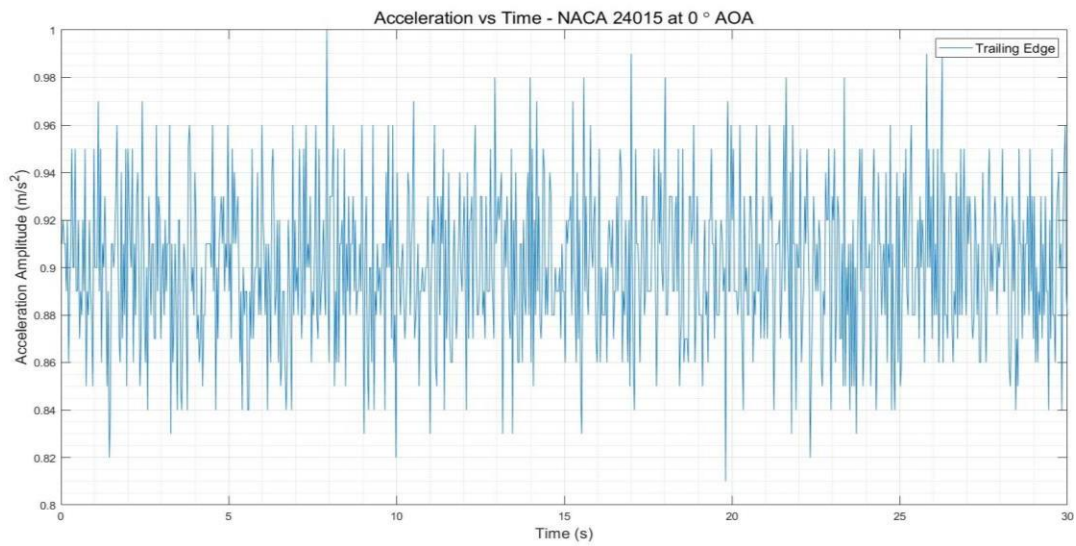


Figure 4.3: NACA 24015- 00 AOA- ACCELERATION VS TIME at 10m/s VELOCITY

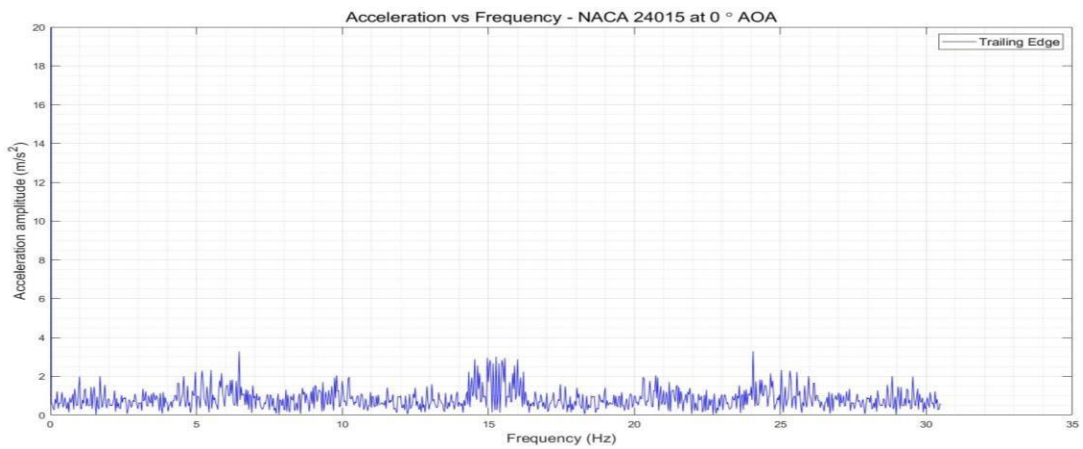


Figure 4.4: NACA 24015- 00 AOA- ACCELERATION VS FREQUENCY at 10m/s VELOCITY

Iteration 3

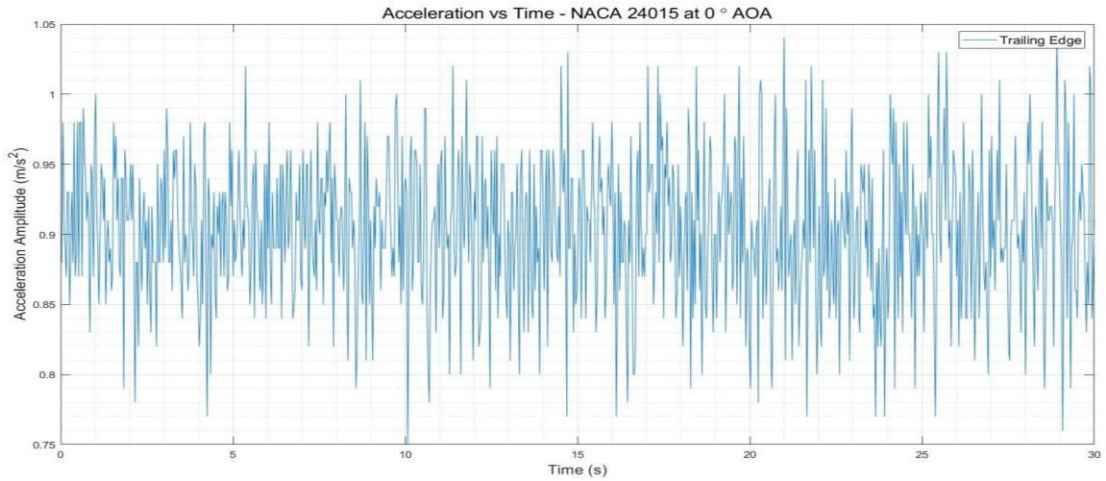


Figure 4.5: NACA 24015- 00 AOA- ACCELERATION VS TIME at 13.7m/s VELOCITY

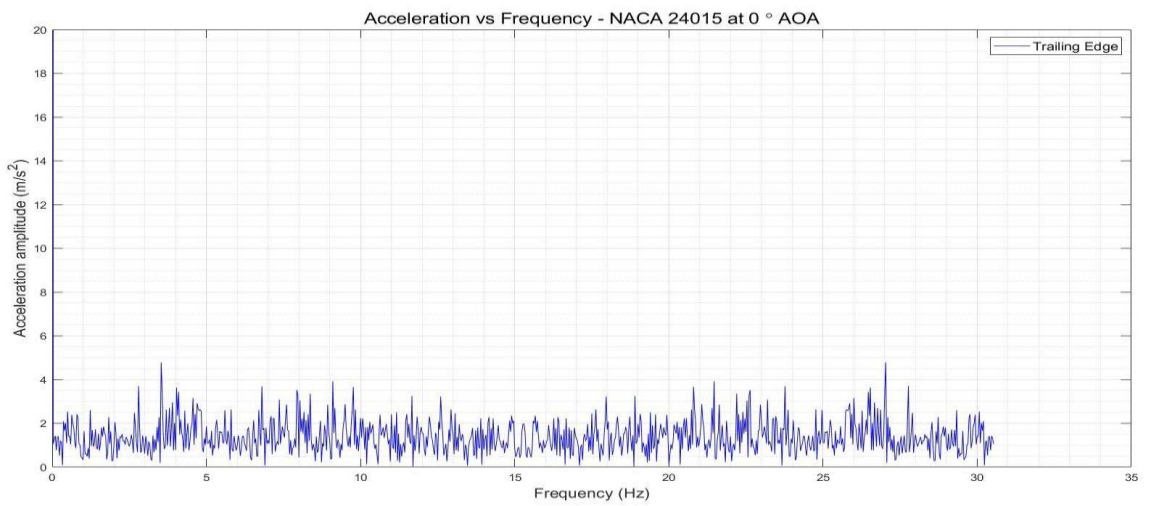


Figure 4.6: NACA 24015- 00 AOA- ACCELERATION VS FREQUENCY at 13.7m/s VELOCITY

Iteration 4

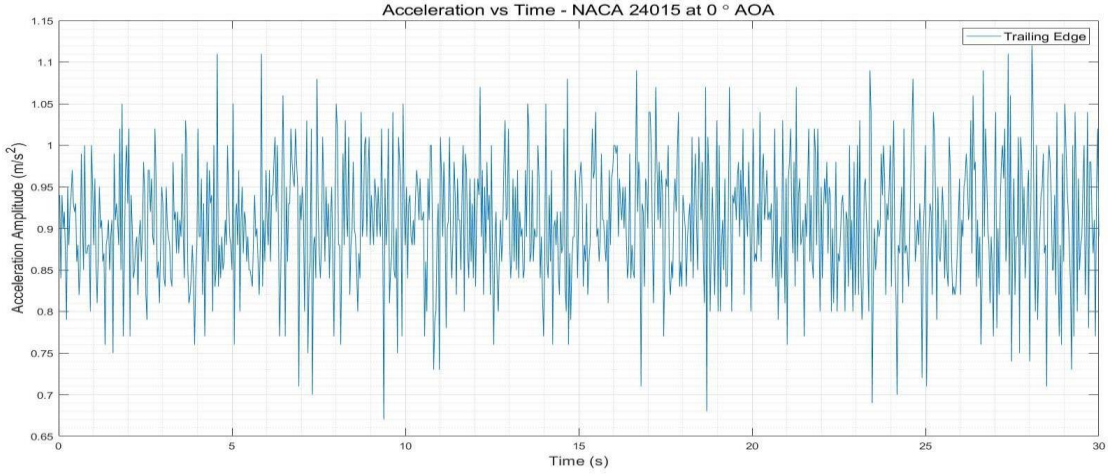


Figure 4.7: NACA 24015- 00 AOA- ACCELERATION VS TIME AT 17.4 m/s VELOCITY

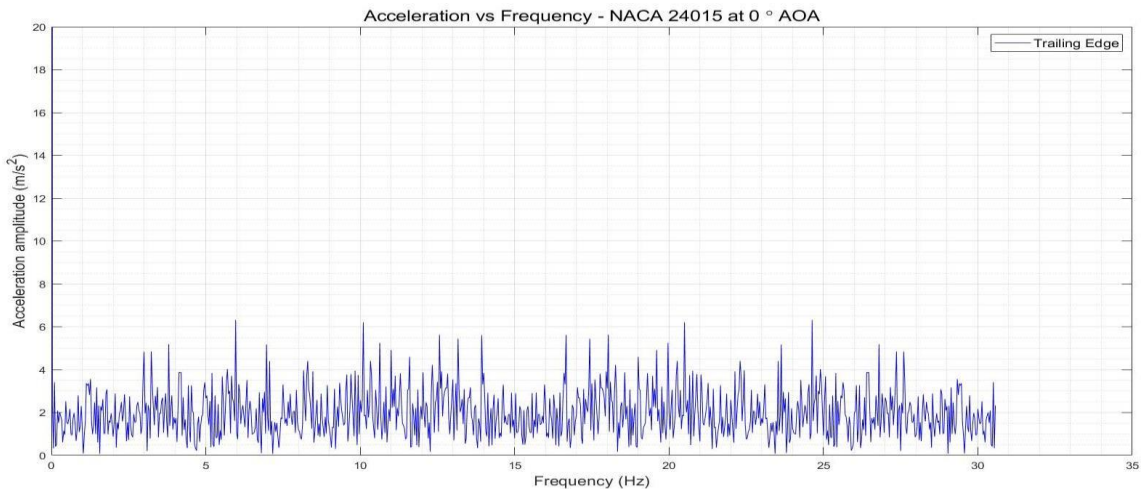


Figure 4.8: NACA 24015- 00 AOA- ACCELERATION VS TIME & FREQUENCY AT 17.4 m/s VELOCITY

Iteration 5

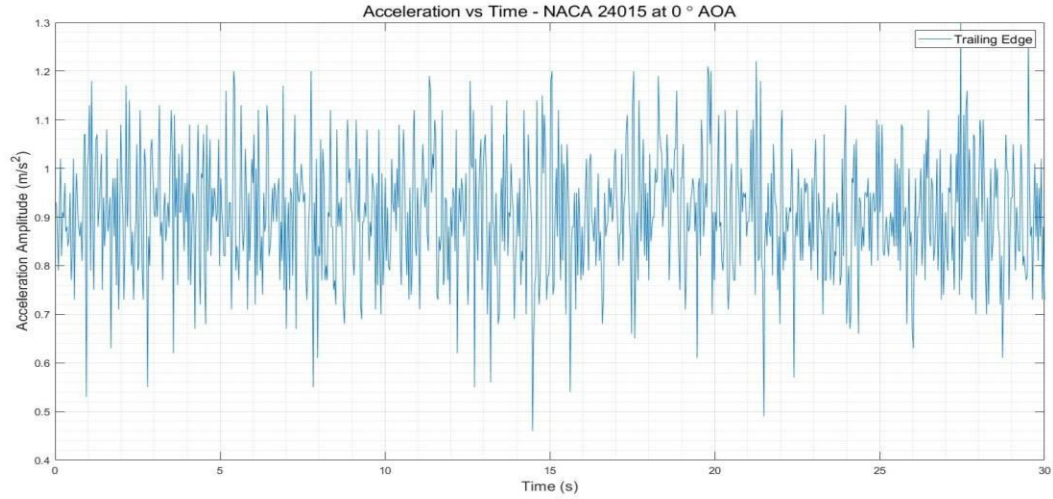


Figure 4.9: NACA 24015- 00 AOA- ACCELERATION VS TIME AT 21.2 m/s VELOCITY

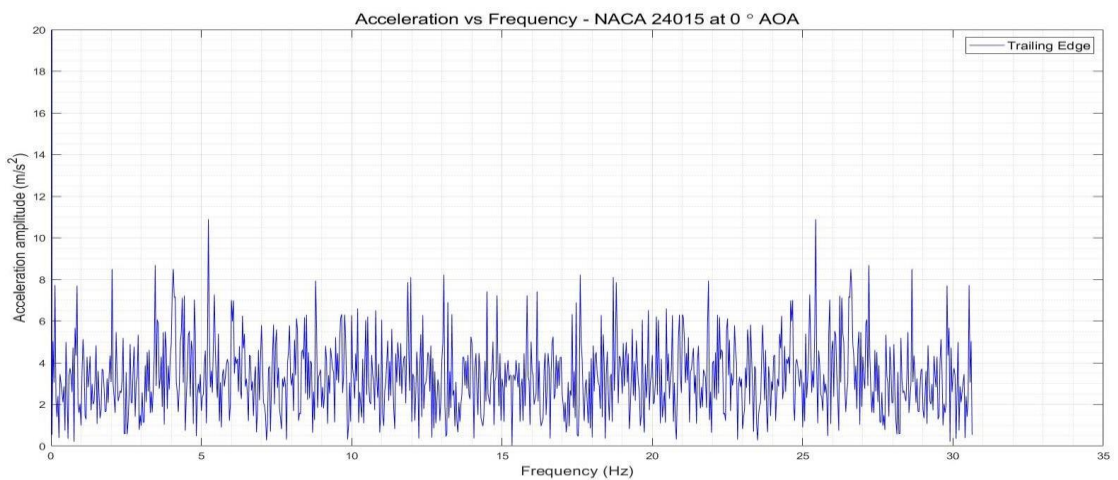


Figure 4.10: NACA 24015- 00 AOA- ACCELERATION VS FREQUENCY AT 21.2 m/s VELOCITY

Iteration 6

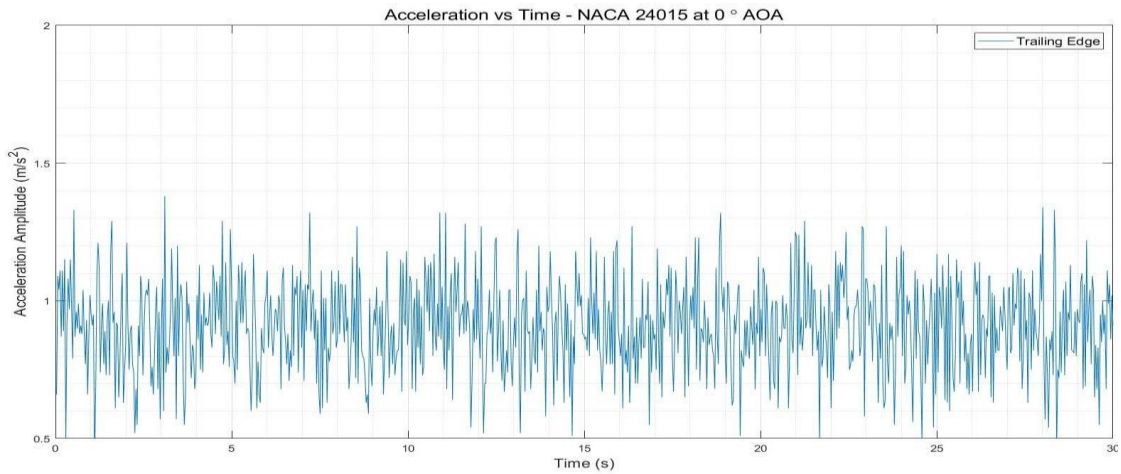


Figure 4.11: NACA 24015- 00 AOA- ACCELERATION VS TIME AT 25.1 m/s VELOCITY

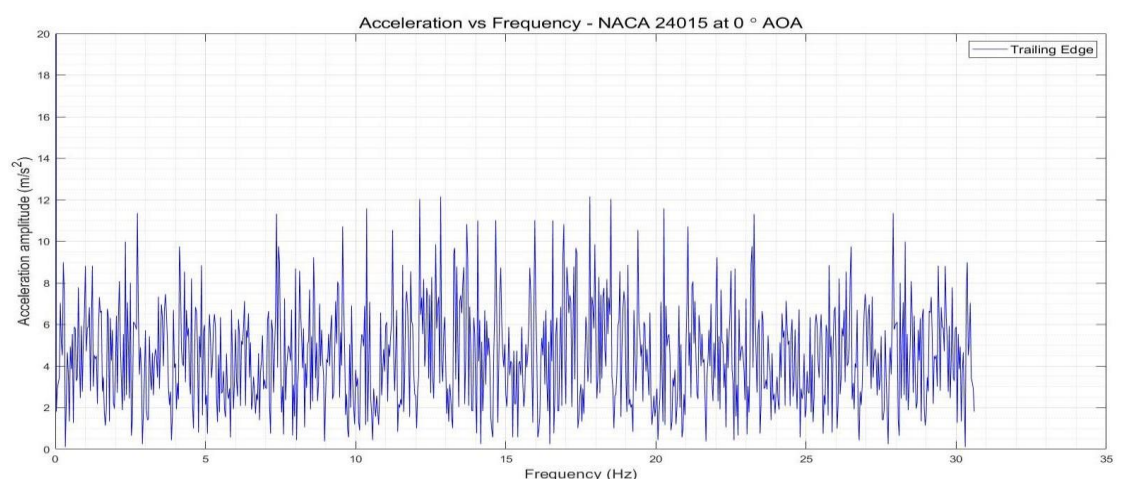


Figure 4.12: NACA 24015- 00 AOA- ACCELERATION VS FREQUENCY AT 25.1 m/s VELOCITY

Iteration 7

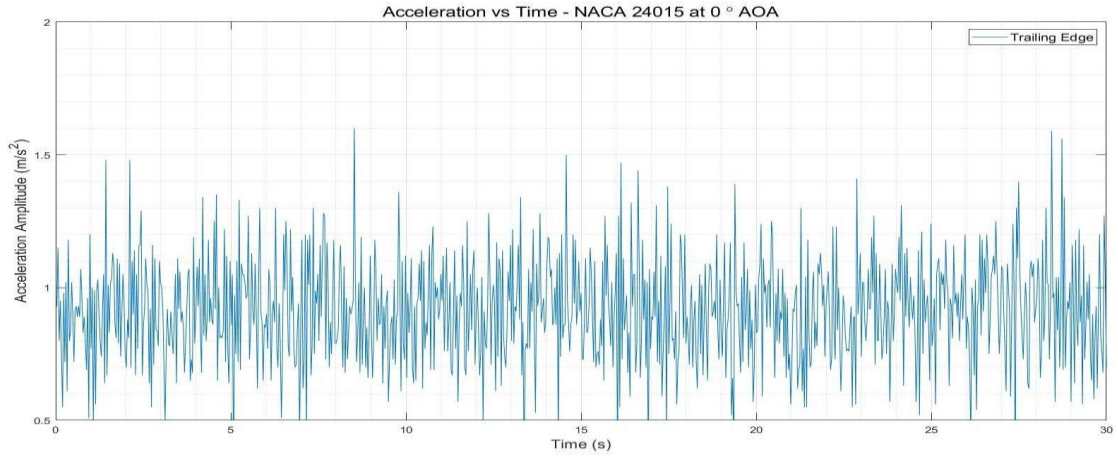


Figure 4.13: NACA 24015- 00 AOA- ACCELERATION VS FREQUENCY & TIME AT 28.8 m/s VELOCITY

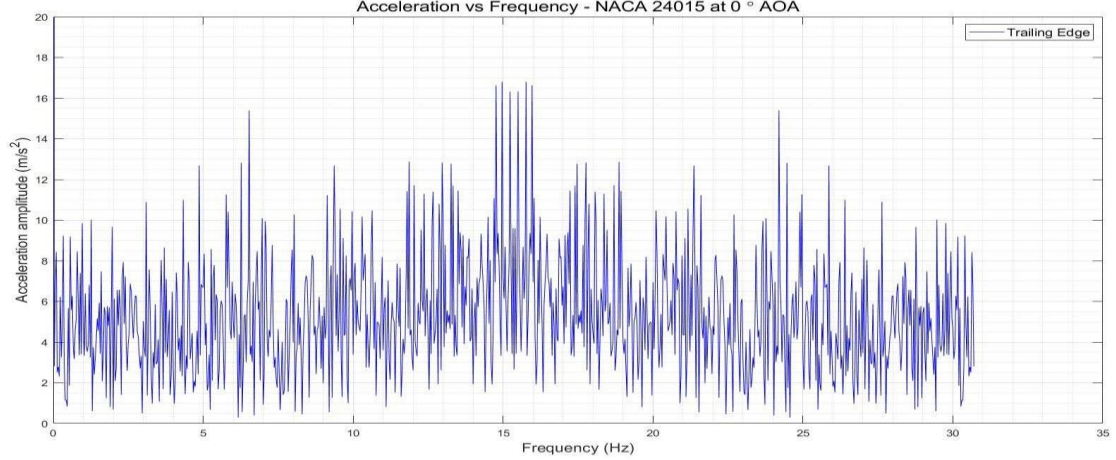


Figure 4.14: NACA 24015- 00 AOA- ACCELERATION VS FREQUENCY AT 28.8 m/s VELOCITY

Iteration 8

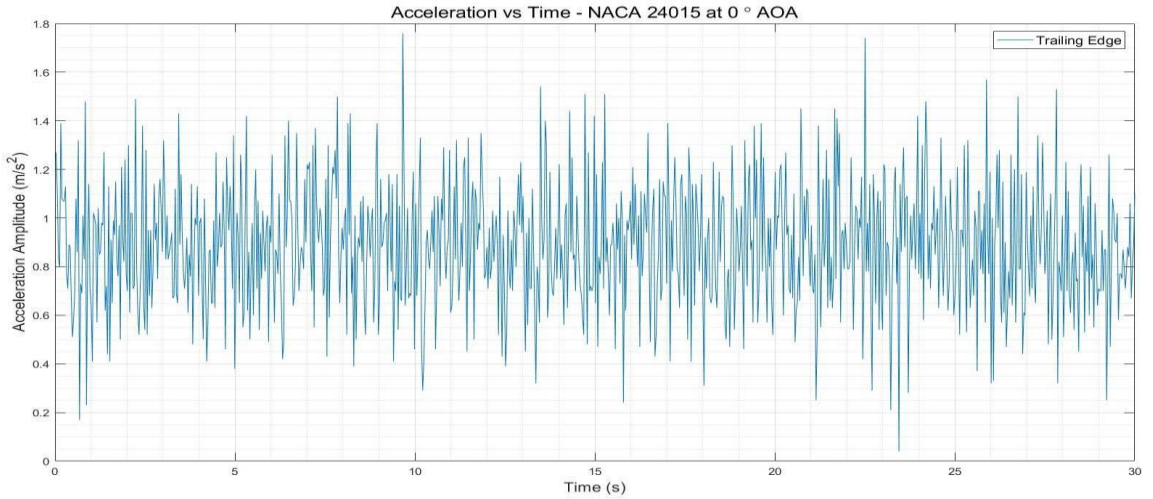


Figure 4.15: NACA 24015- 00 AOA- ACCELERATION VS TIME AT 32.7 m/s VELOCITY

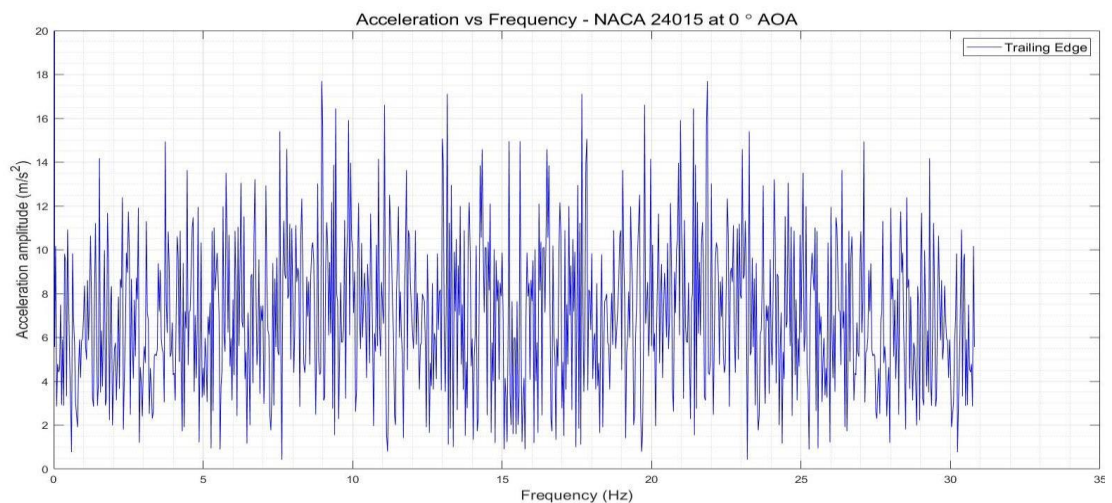


Figure 4.16: NACA 24015- 00 AOA- ACCELERATION VS FREQUENCY AT 32.7 m/s VELOCITY

Iteration 9

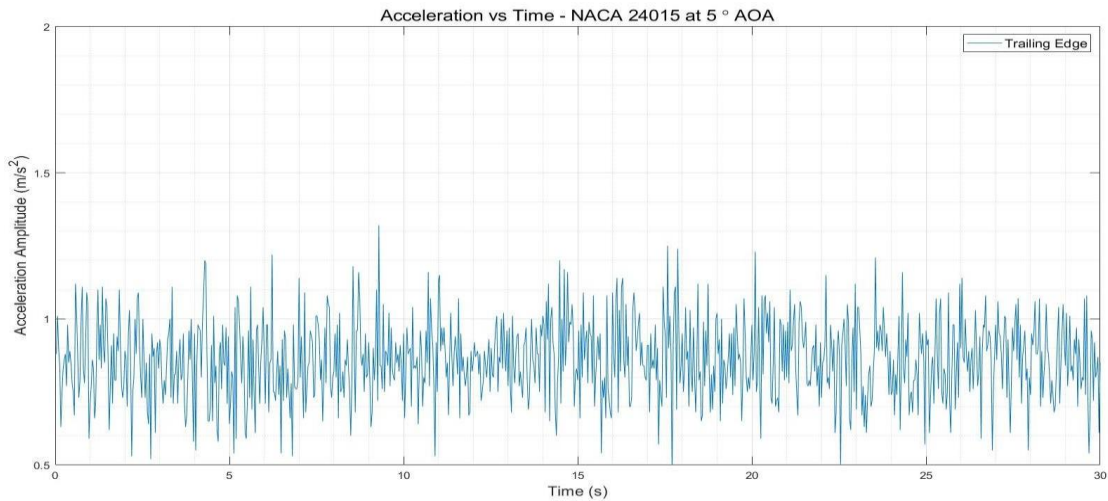


Figure 4.17: NACA 24015- 50 AOA- ACCELERATION VS TIME

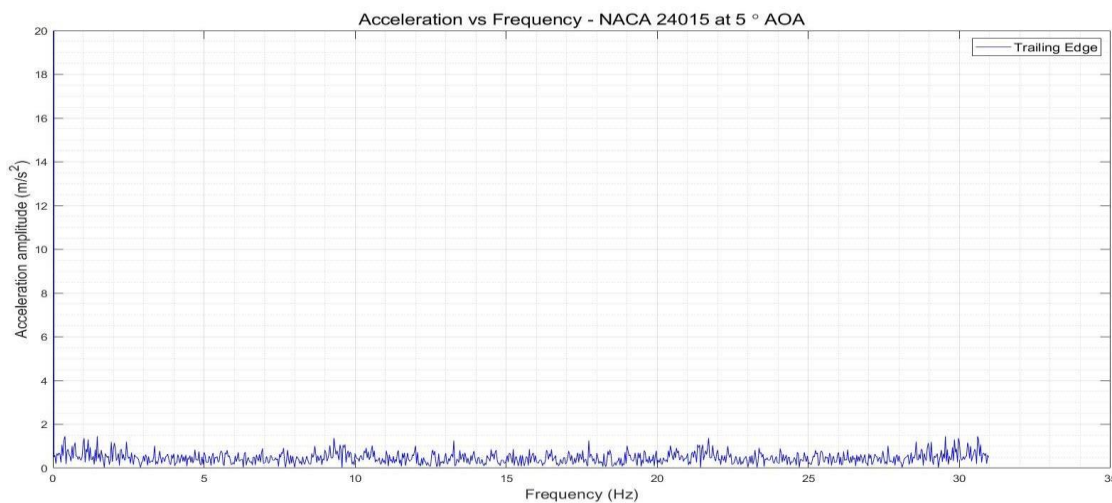


Figure 4.18: NACA 24015- 50 AOA- ACCELERATION VS FREQUENCY AT

Iteration 10

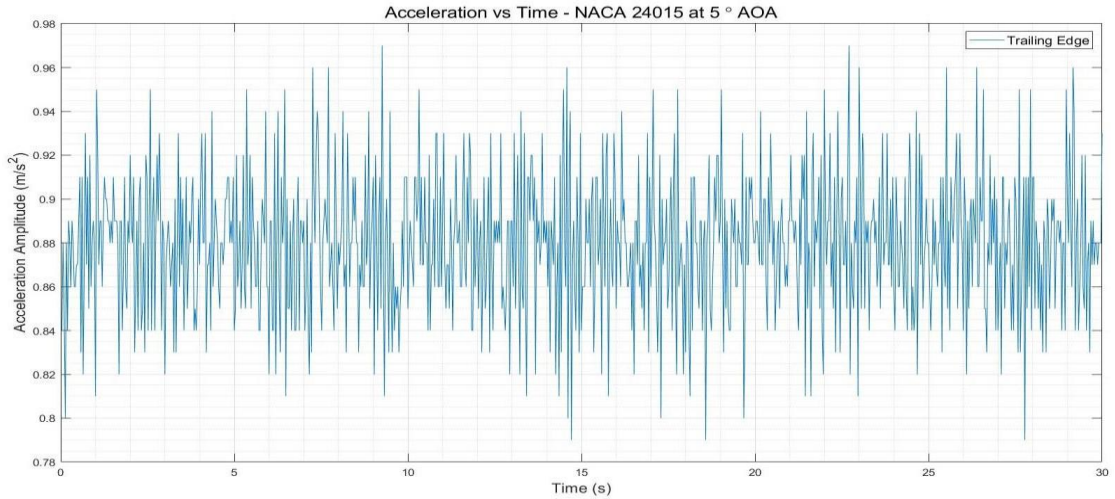


Figure 4.19: NACA 24015- 50 AOA- ACCELERATION VS TIME AT 10 m/s VELOCITY

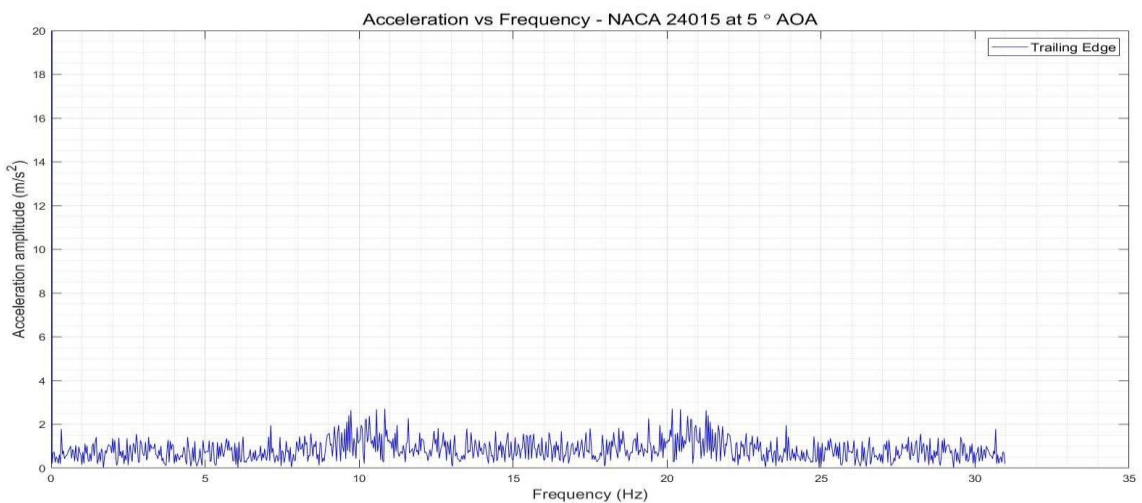


Figure 4.20: NACA 24015- 50 AOA- ACCELERATION VS FREQUENCY AT 10 m/s VELOCITY

Iteration 11

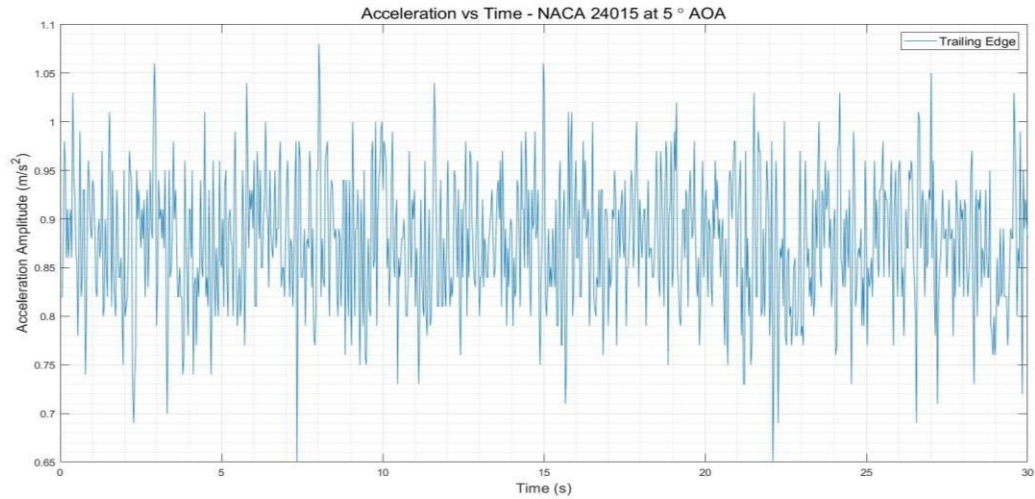


Figure 4.21: NACA 24015- 50 AOA- ACCELERATION VS TIME AT 13.7 m/s VELOCITY

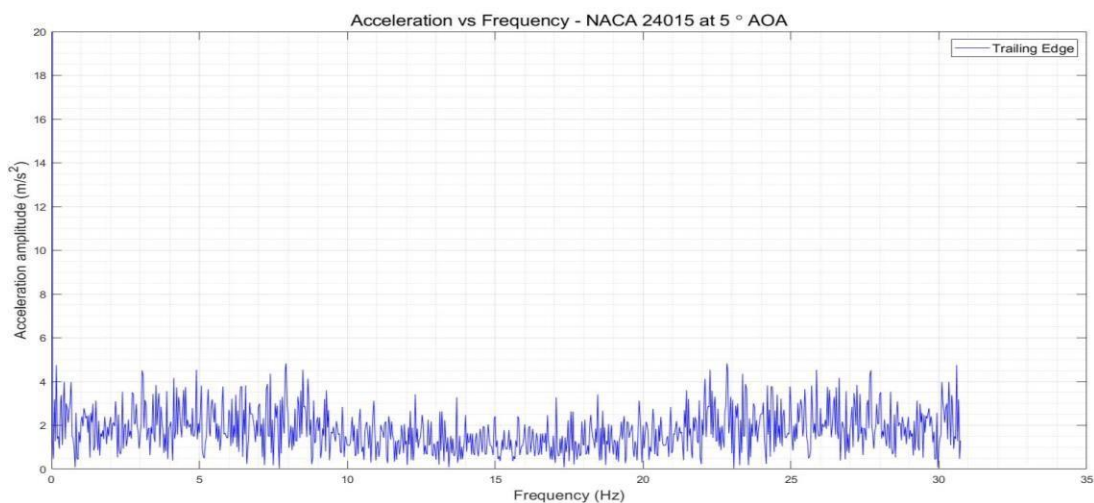


Figure 4.22: NACA 24015- 50 AOA- ACCELERATION VS FREQUENCY AT 13.7 m/s VELOCITY

Iteration 12

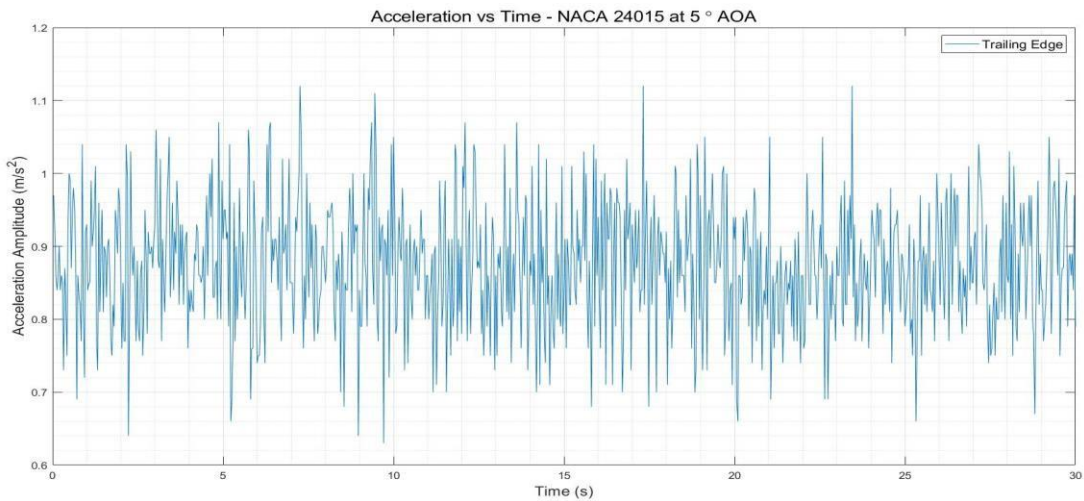


Figure 4.23: NACA 24015- 50 AOA- ACCELERATION VS TIME AT 17.4 m/s VELOCITY

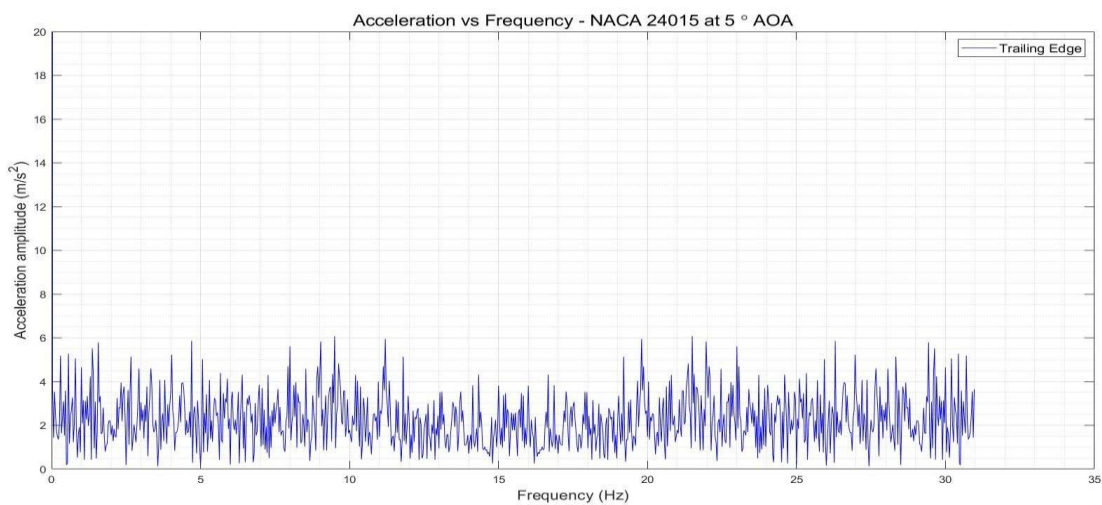


Figure 4.24: NACA 24015- 50 AOA- ACCELERATION VS FREQUENCY AT 17.4 m/s VELOCITY

Iteration 13

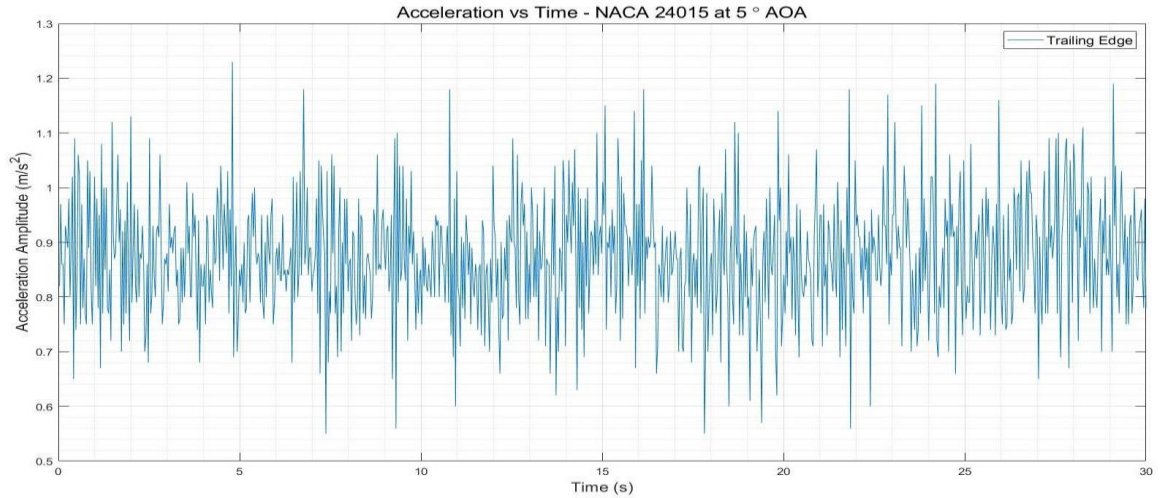


Figure 4.25: NACA 24015- 50 AOA- ACCELERATION VS TIME AT 21.2 m/s VELOCITY

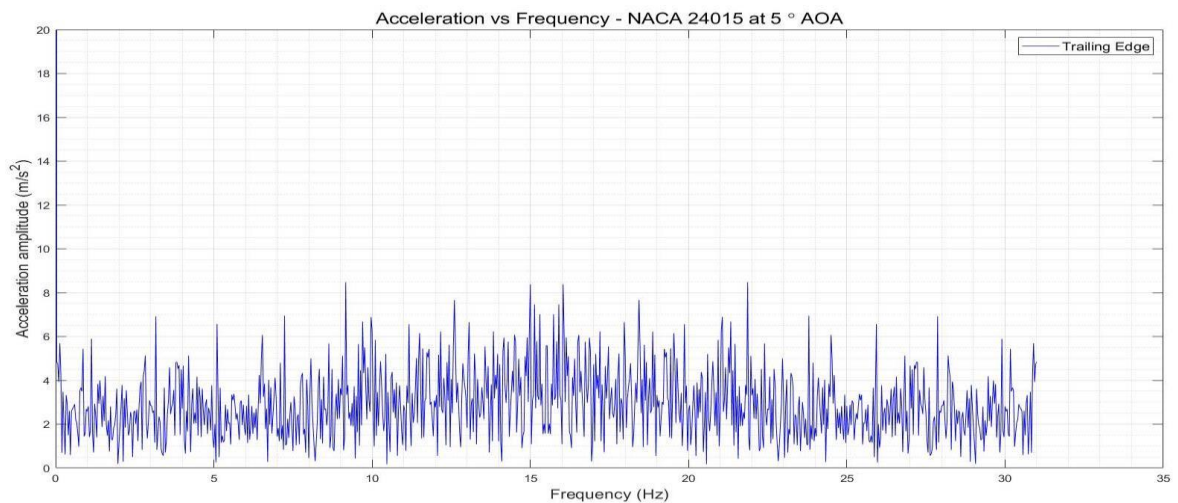


Figure 4.26: NACA 24015- 50 AOA- ACCELERATION VS FREQUENCY AT 21.2 m/s VELOCITY

Iteration 14

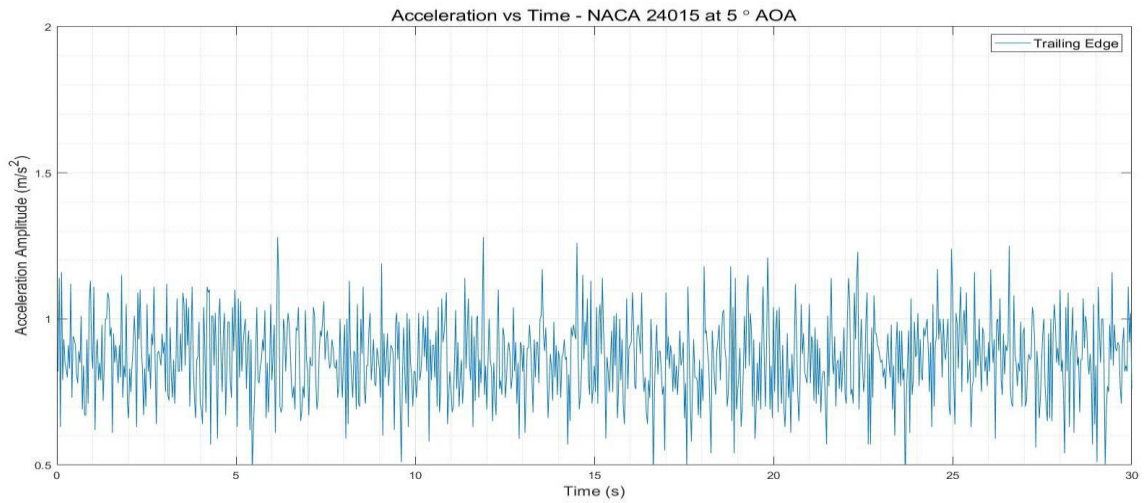


Figure 4.27: NACA 24015- 50 AOA- ACCELERATION VS TIME AT 25.1 m/s VELOCITY

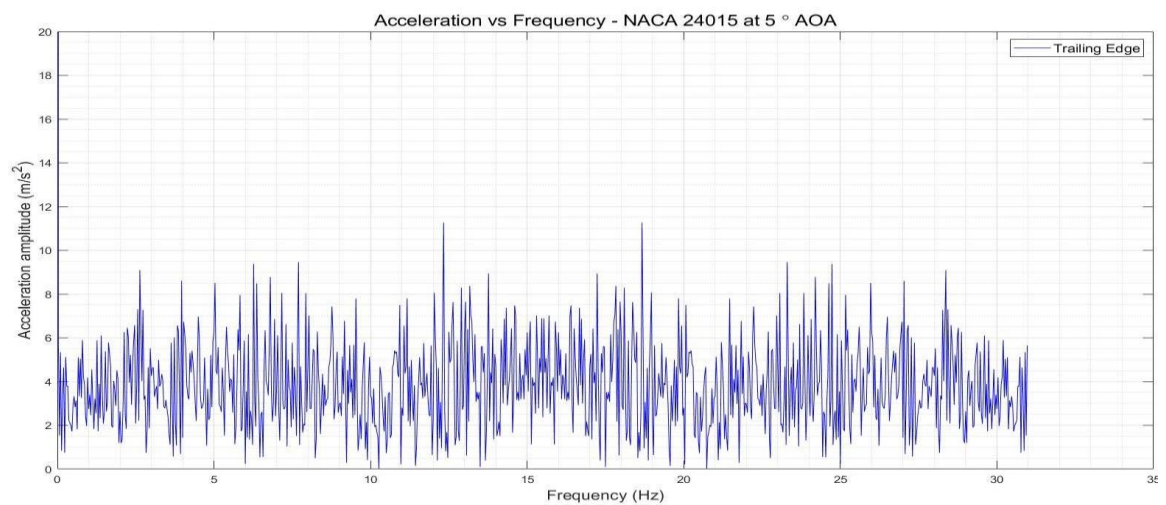


Figure 4.28: NACA 24015- 50 AOA- ACCELERATION VS FREQUENCY AT 25.1 m/s VELOCITY

Iteration 15

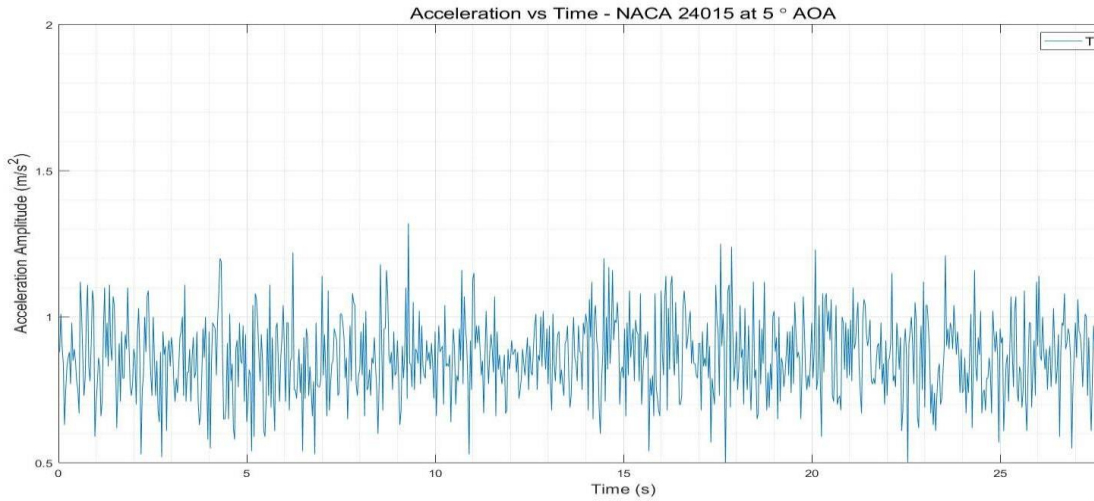


Figure 4.29: NACA 24015- 50 AOA- ACCELERATION VS TIME AT 28.8m/s VELOCITY

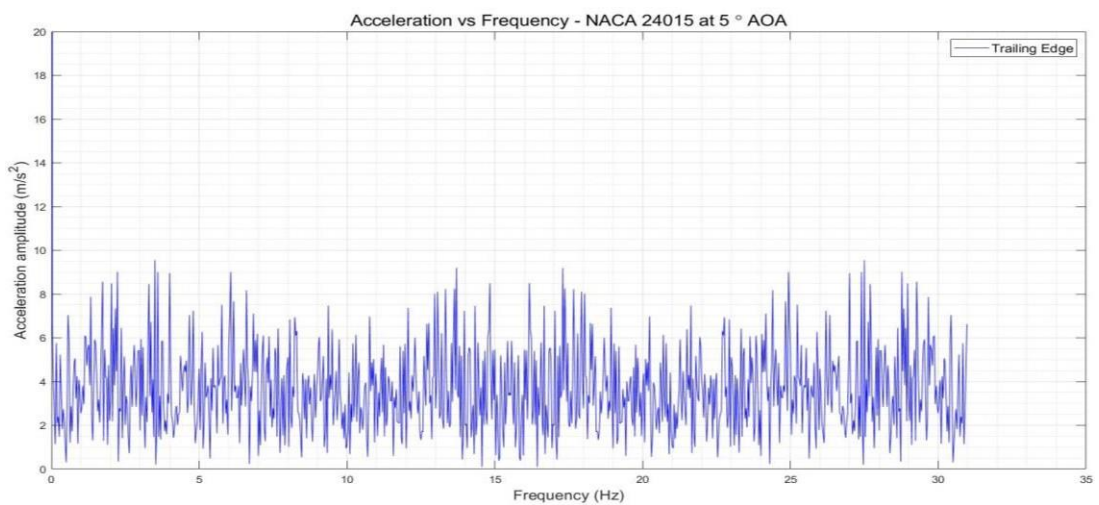


Figure 4.30: NACA 24015- 50 AOA- ACCELERATION VS FREQUENCY AT 28.8 m/s VELOCITY

Iteration 16

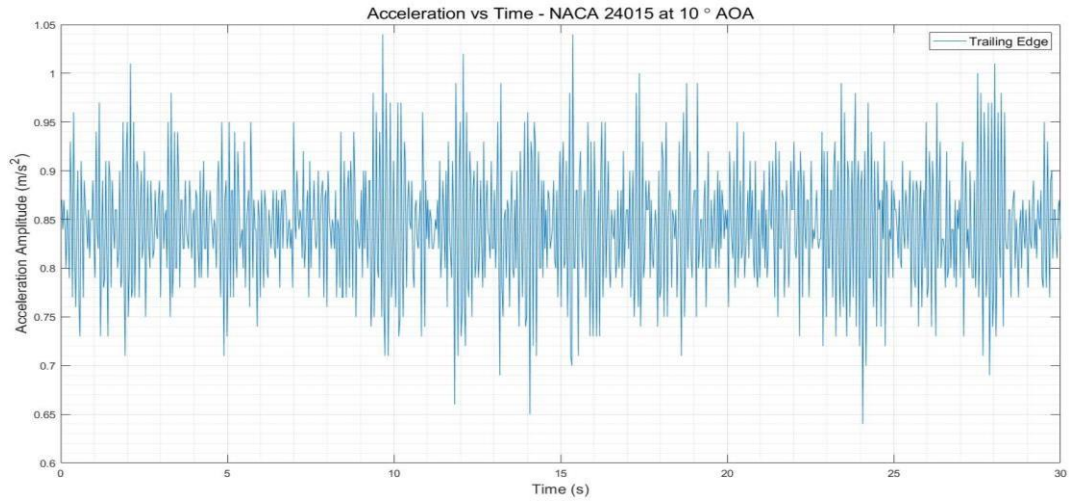


Figure 4.31: NACA 24015- 100 AOA- ACCELERATION VS TIME AT 6.37 m/s VELOCITY.

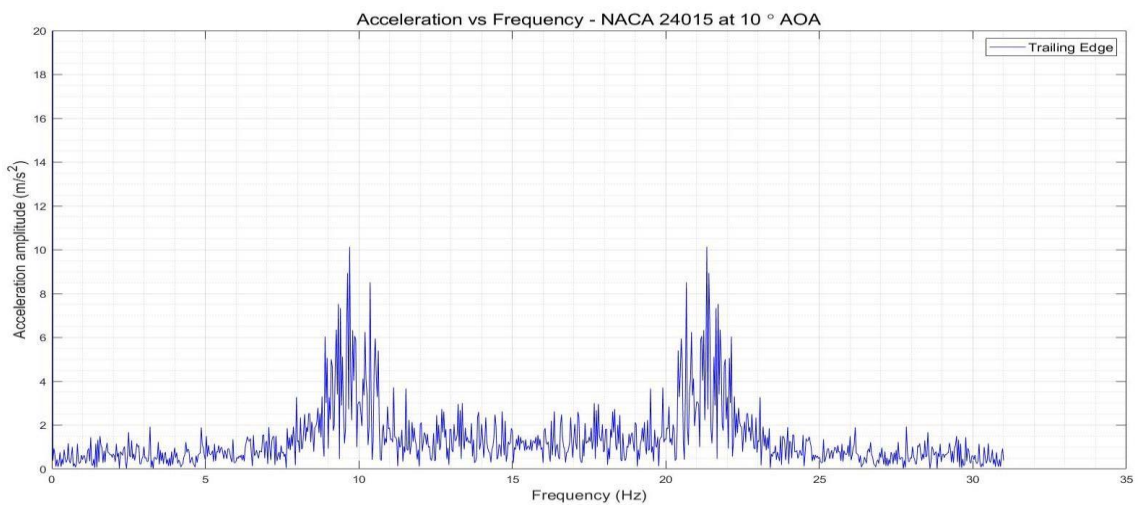


Figure 4.32: NACA 24015- 100 AOA- ACCELERATION VS FREQUENCY AT 6.37 m/s VELOCITY

Iteration 17

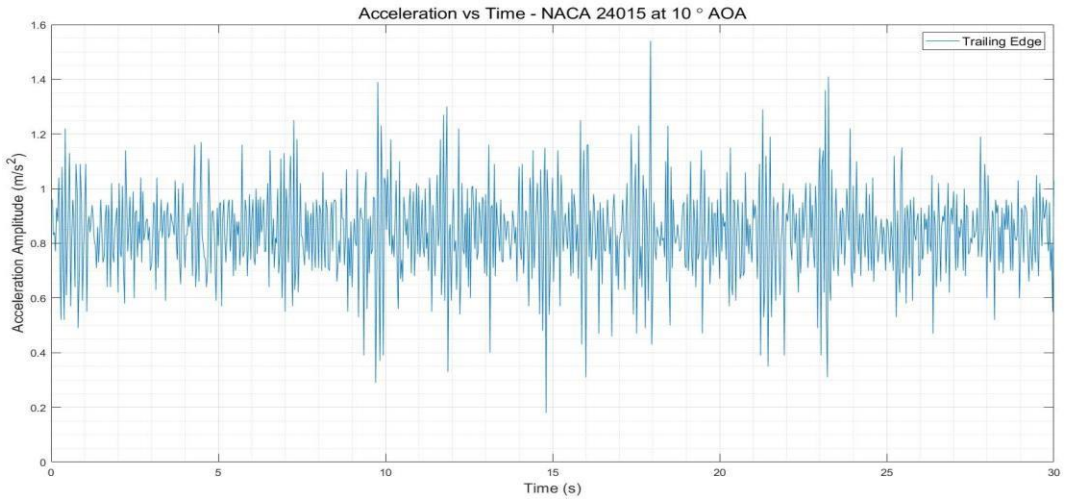


Figure 4.34: NACA 24015- 100 AOA- ACCELERATION VS TIME AT 10 m/s VELOCITY

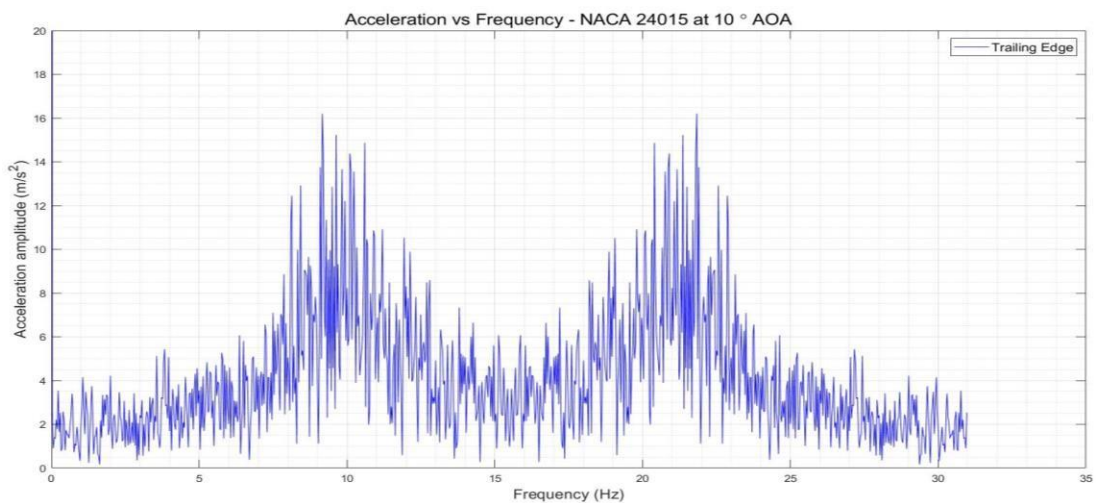


Figure 4.33: NACA 24015- 100 AOA- ACCELERATION VS FREQUENCY AT 10 m/s VELOCITY

Iteration 18

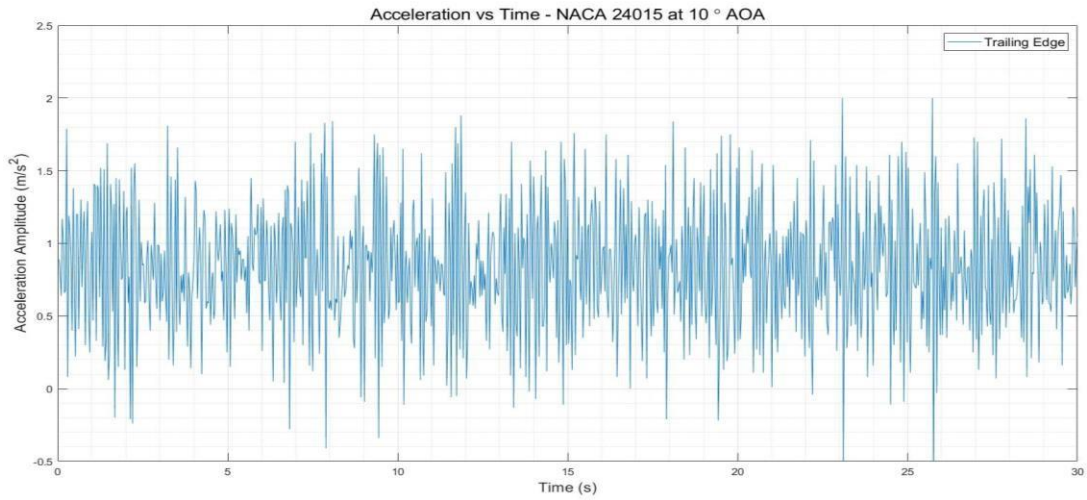


Figure 4.35: NACA 24015- 100 AOA- ACCELERATION VS TIME AT 13.7 m/s VELOCITY

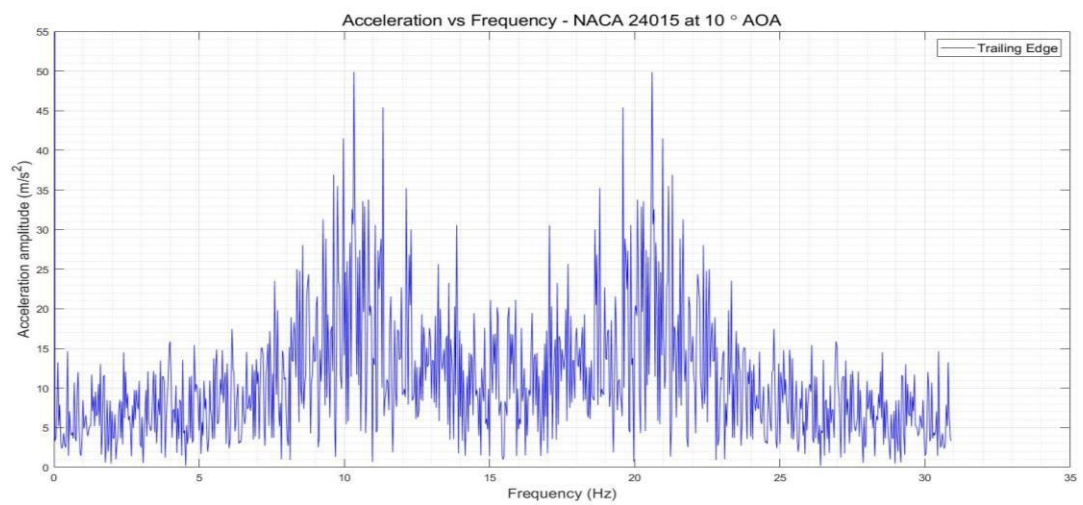


Figure 4.36: NACA 24015- 100 AOA- ACCELERATION VS FREQUENCY AT 13.7 m/s VELOCITY

ITERATION 19

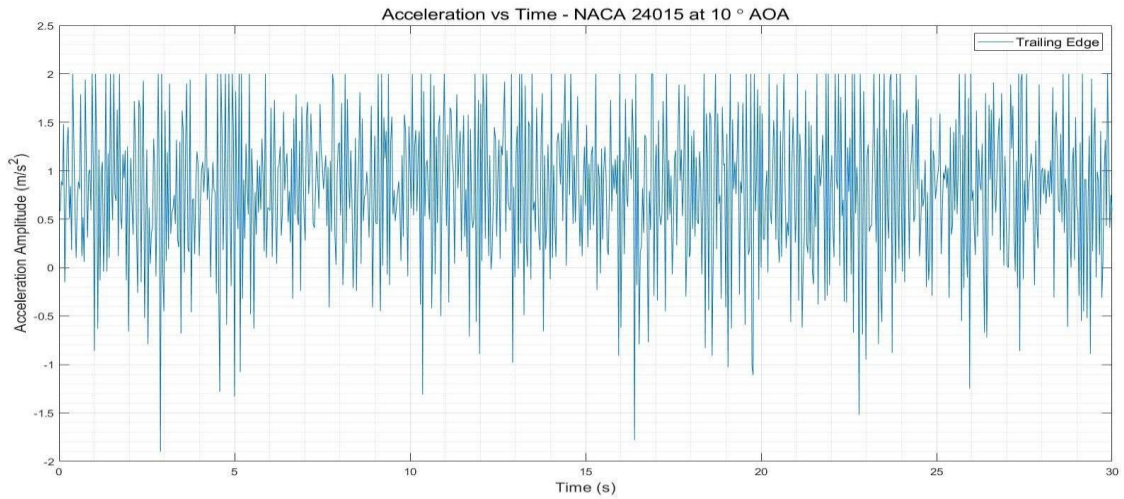


Figure 4.37: NACA 24015- 100 AOA- ACCELERATION VS TIME AT 17.4 m/s VELOCITY

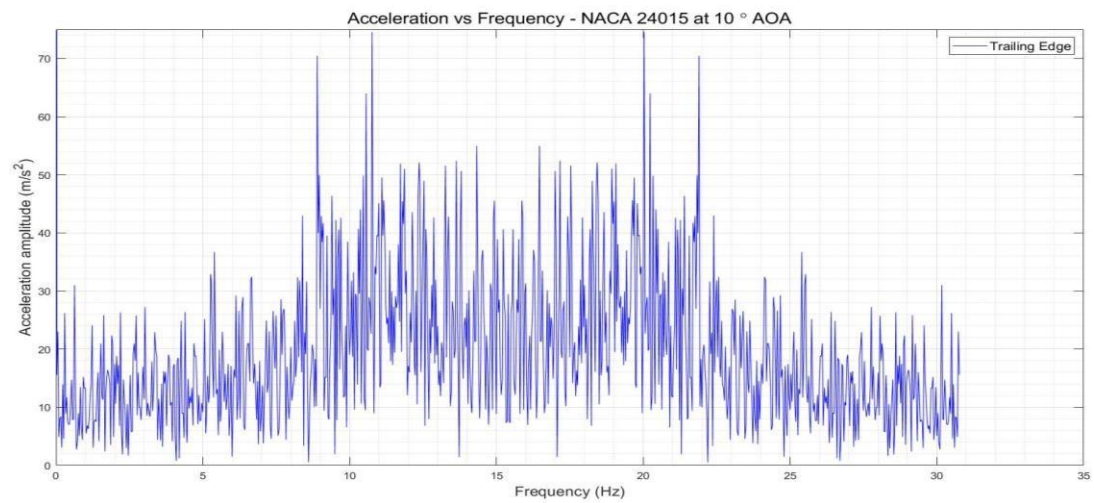


Figure 4.38: NACA 24015- 100 AOA- ACCELERATION VS FREQUENCY AT 17.4 m/s VELOCITY

ITERATION 20

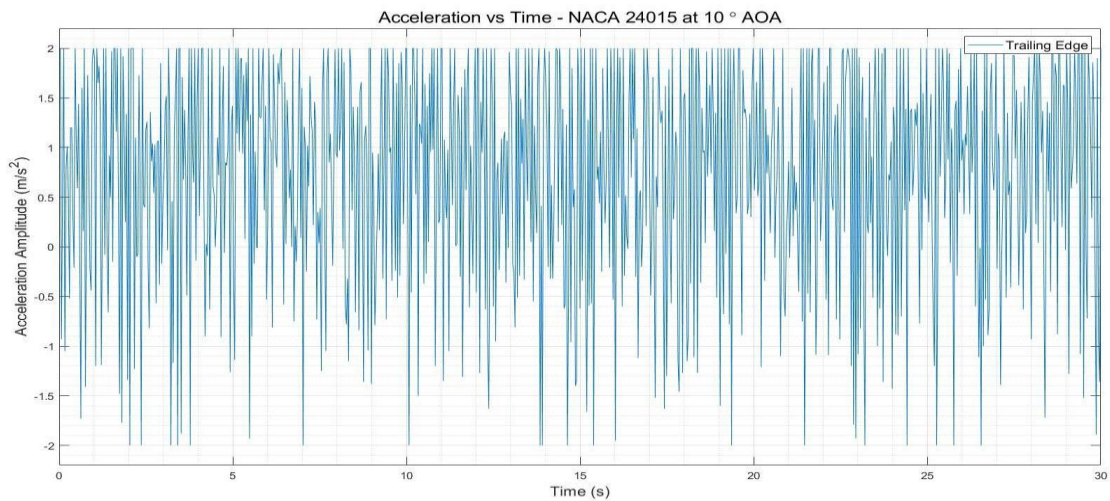


Figure 4.39: NACA 24015- 100 AOA- ACCELERATION VS TIME AT 21.2 m/s VELOCITY

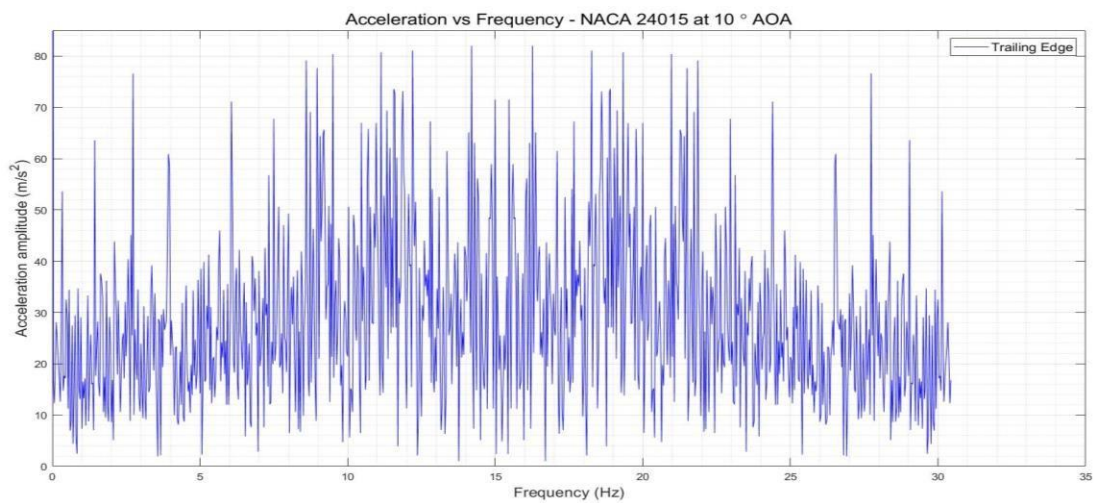


Figure 4.40: NACA 24015- 100 AOA- ACCELERATION VS FREQUENCY AT 21.2 m/s VELOCITY

ITERATION 21

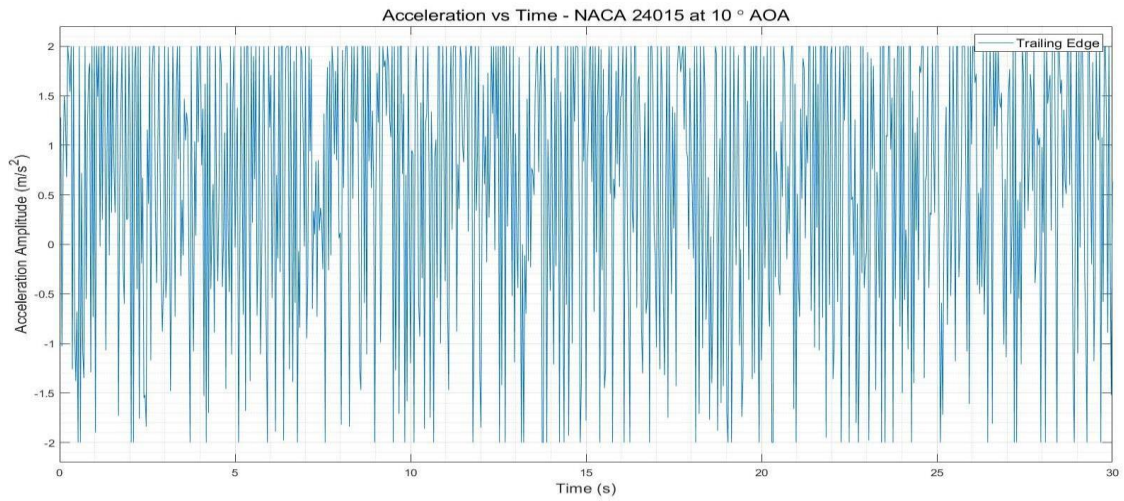


Figure 4.41: NACA 24015- 100 AOA- ACCELERATION VS TIME AT 25.1m/s VELOCITY

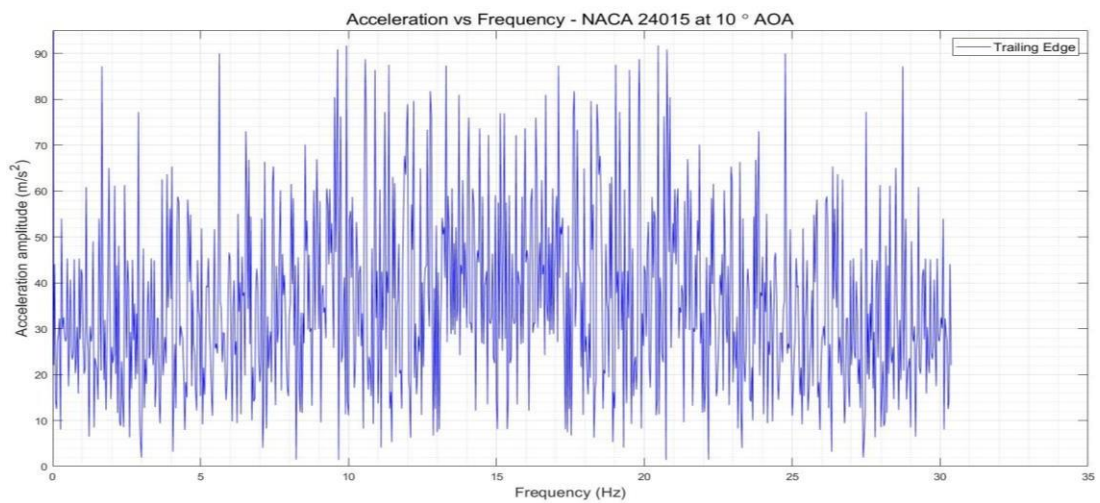


Figure 4.42: NACA 24015- 100 AOA- ACCELERATION VS FREQUENCY AT 25.1m/s VELOCITY

ITERATION 22

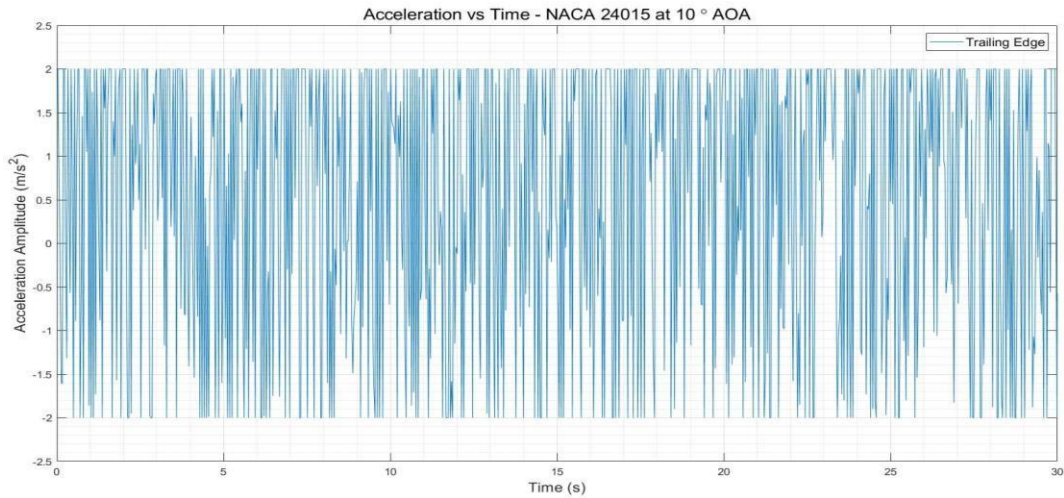


Figure 4.43: NACA 24015- 100 AOA- ACCELERATION VS TIME AT 28.8m/s VELOCITY

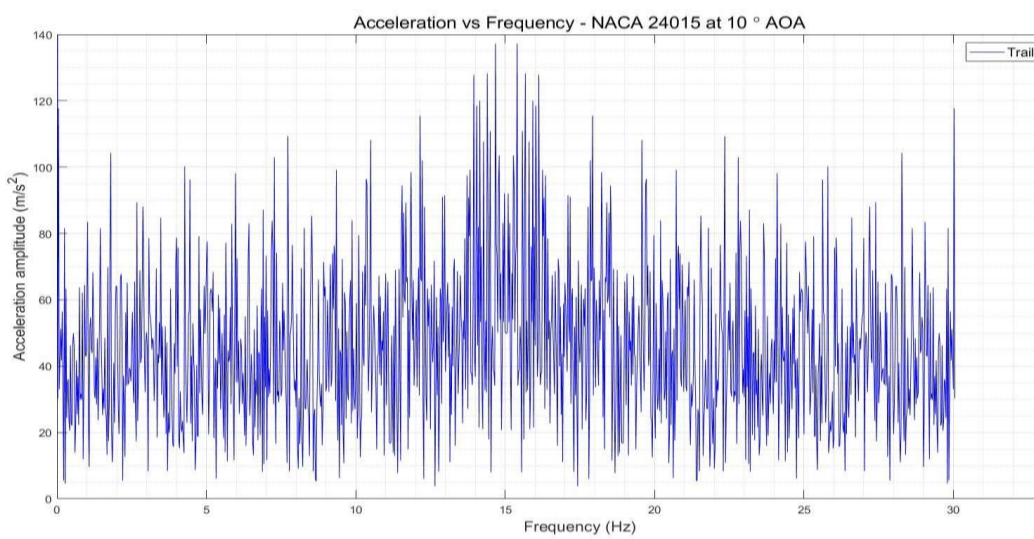


Figure 4.44: NACA 24015- 100 AOA- ACCELERATION VS FREQUENCY AT 28.8m/s VELOCITY

ITERATION 23

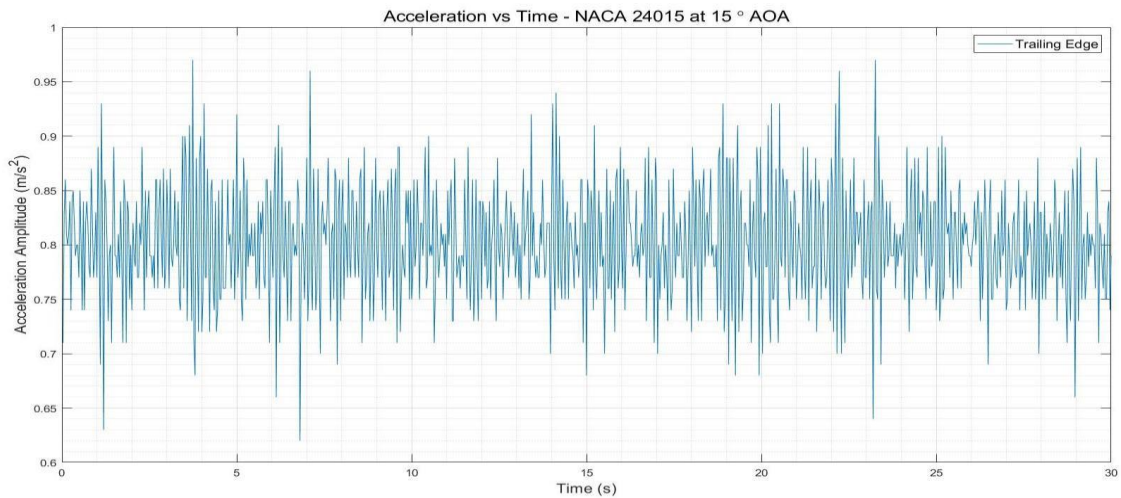


Figure 4.45: NACA 24015- 150 AOA- ACCELERATION VS TIME AT 6.37 m/s VELOCITY

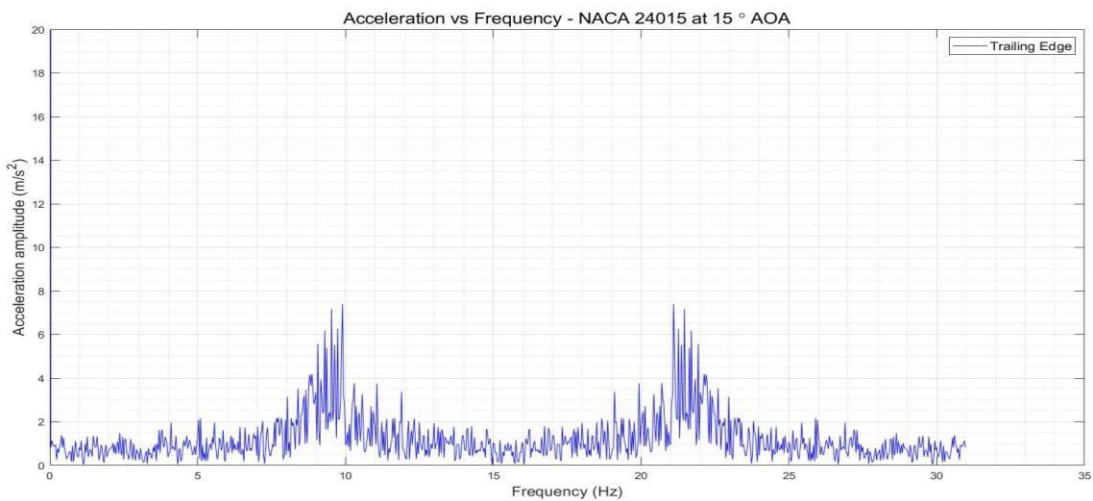


Figure 4.46: NACA 24015- 150 AOA- ACCELERATION VS FREQUENCY AT 6.37 m/s VELOCITY

ITERATION 24

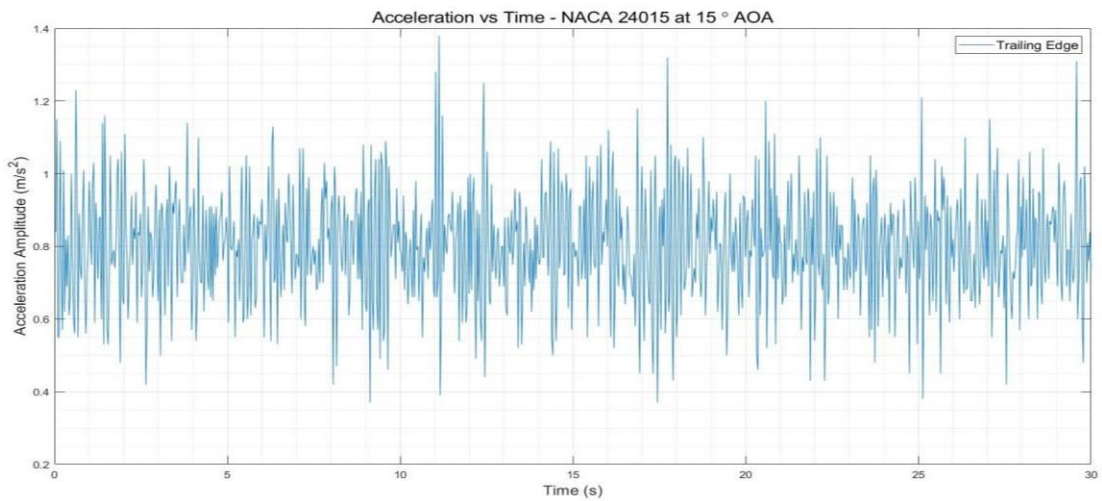


Figure 4.47: NACA 24015- 150 AOA- ACCELERATION VS TIME AT 10 m/s VELOCITY

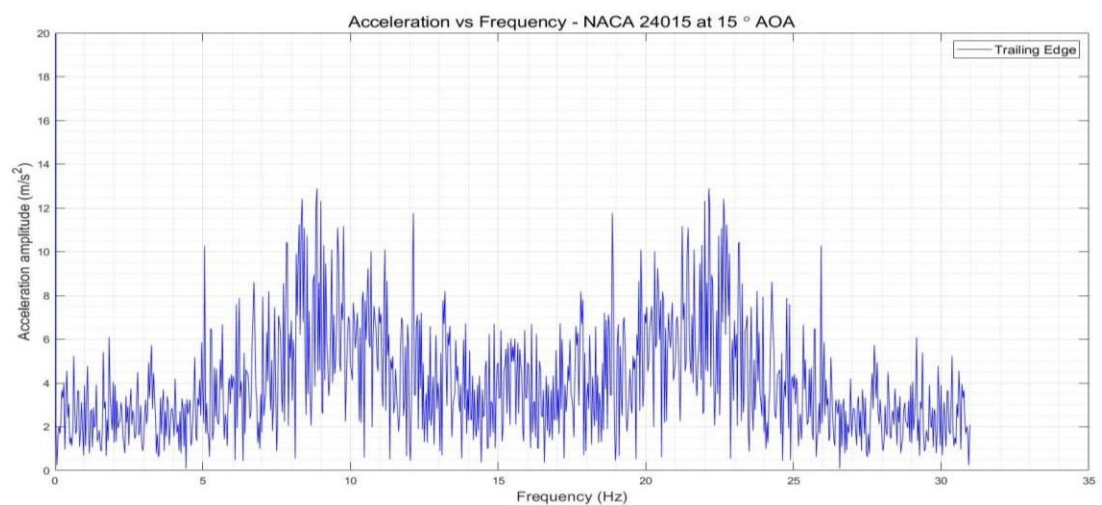


Figure 4.48: NACA 24015- 150 AOA- ACCELERATION VS FREQUENCY AT 10 m/s VELOCITY

ITERATION 25

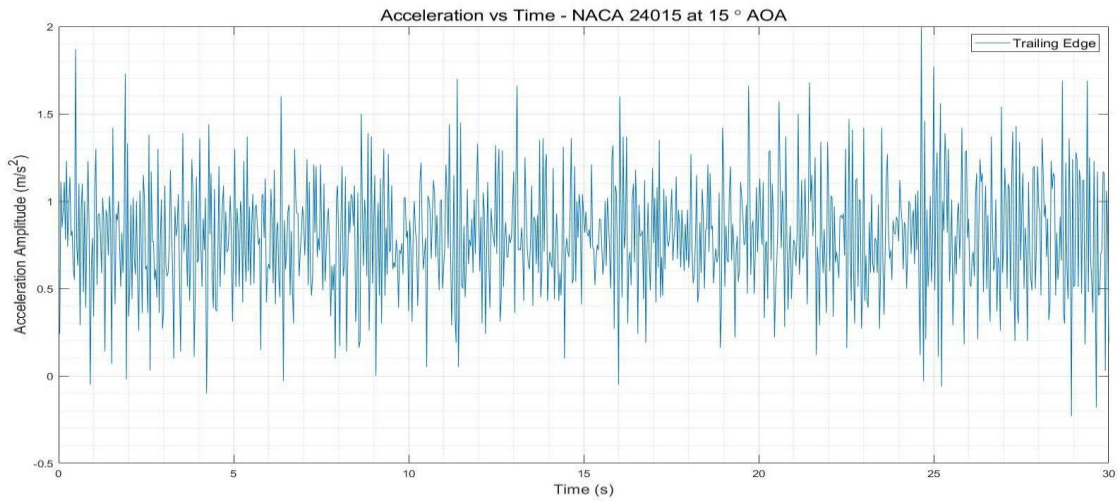


Figure 4.49: NACA 24015- 150 AOA- ACCELERATION VS TIME AT 13.7 m/s VELOCITY

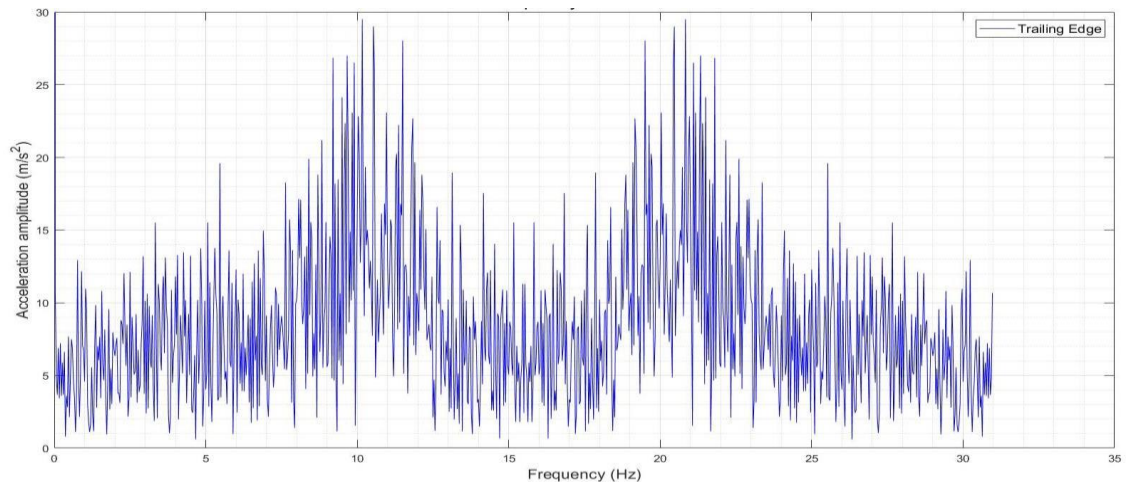


Figure 4.50: NACA 24015- 150 AOA- ACCELERATION VS FREQUENCY AT 13.7 m/s VELOCITY

ITERATION 26

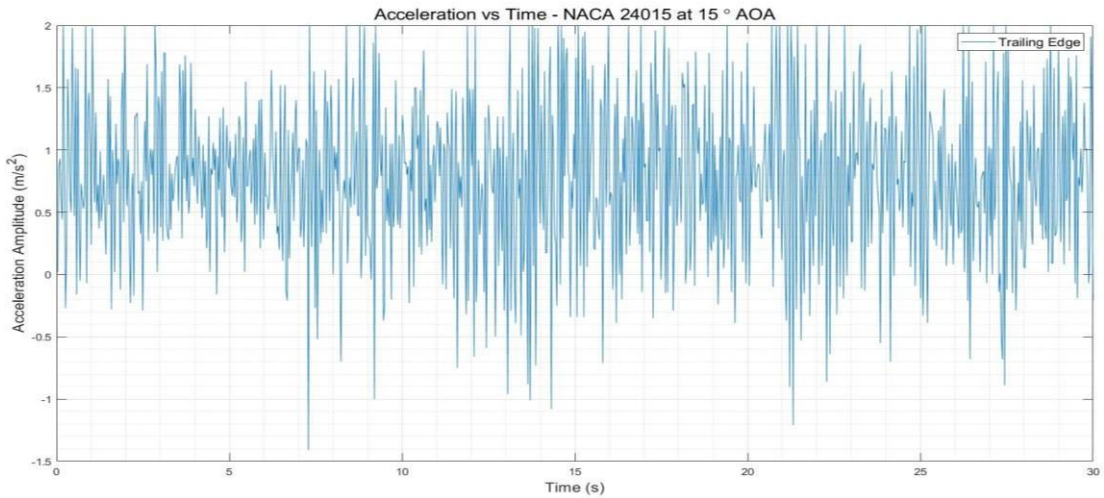


Figure 4.51: NACA 24015- 150 AOA- ACCELERATION VS TIME AT 17.4 m/s VELOCITY

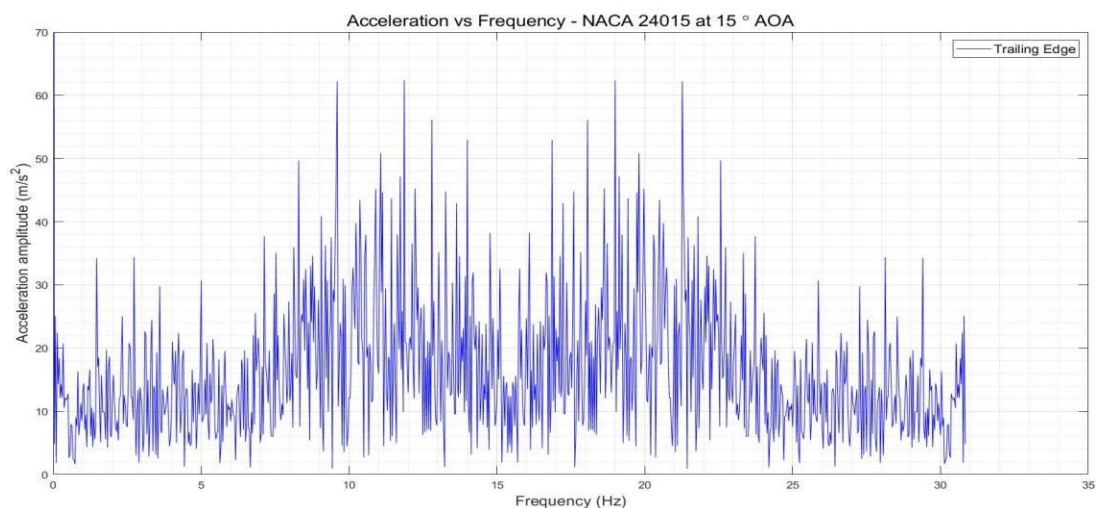


Figure 4.52: NACA 24015- 150 AOA- ACCELERATION VS FREQUENCY AT 17.4 m/s VELOCITY

ITERATION 27

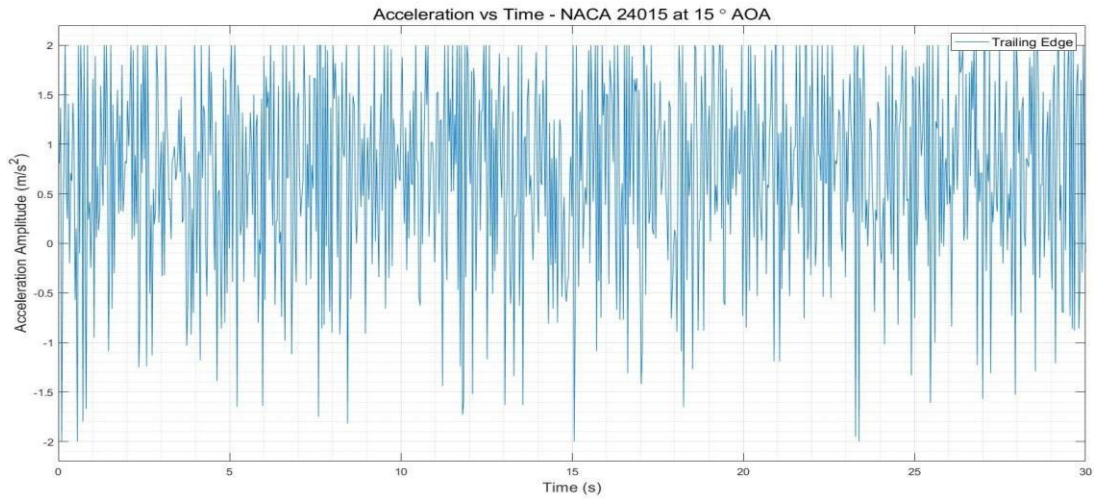


Figure 4.53: NACA 24015- 150 AOA- ACCELERATION VS TIME AT 21.2 m/s VELOCITY

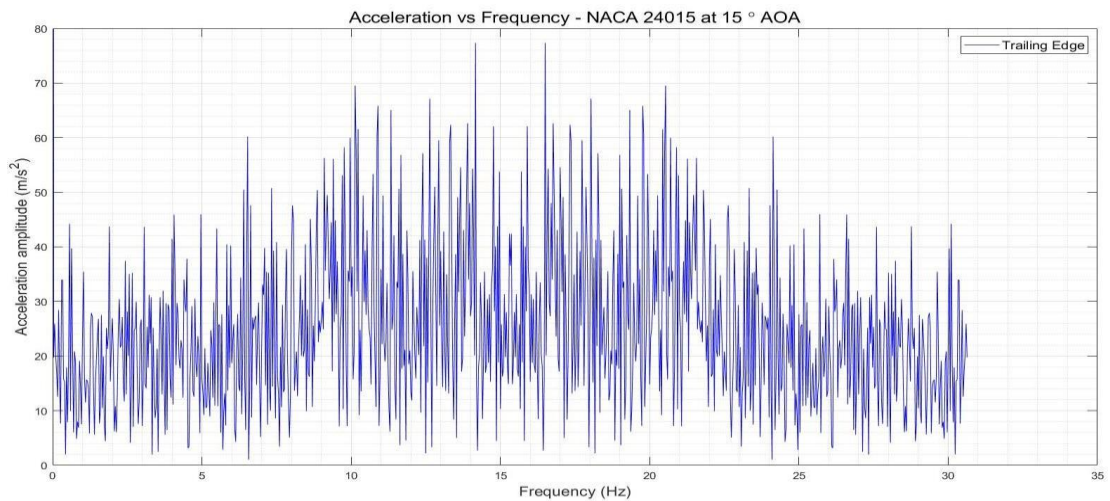


Figure 4.54: NACA 24015- 150 AOA- ACCELERATION VS FREQUENCY AT 21.2 m/s VELOCITY

ITERATION 28

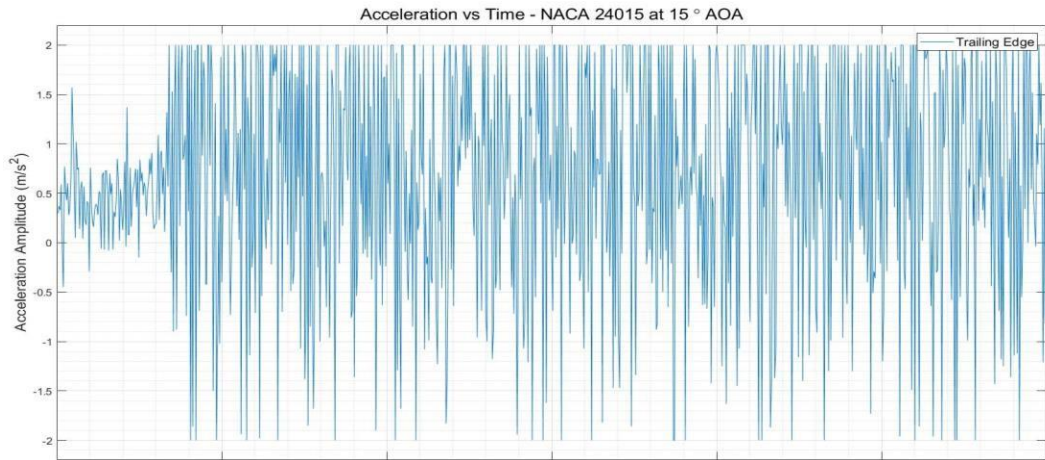


Figure 4.55: NACA 24015- 150 AOA- ACCELERATION VS TIME AT 25.1 m/s VELOCITY

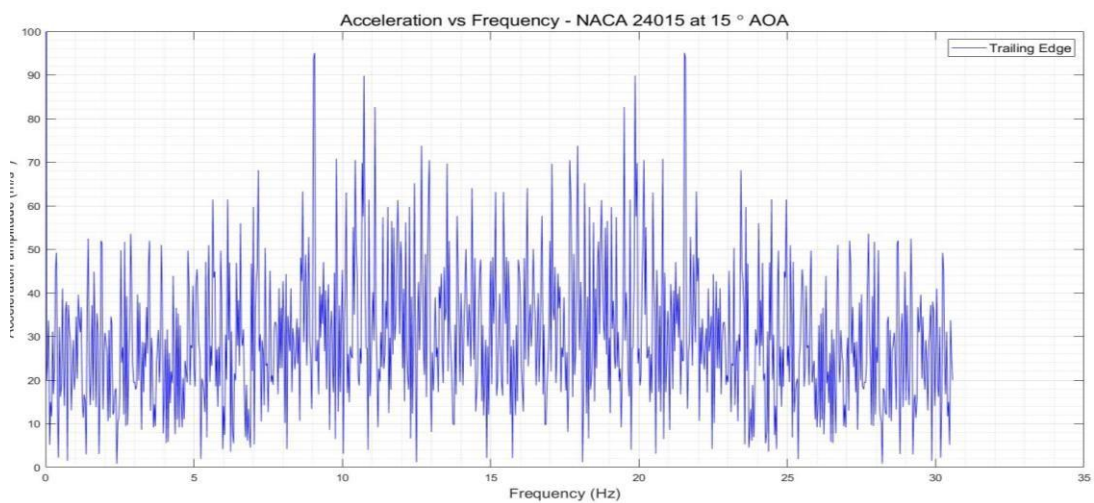


Figure 4.56: NACA 24015- 150 AOA- ACCELERATION VS FREQUENCY AT 25.1 m/s VELOCITY

ITERATION 29

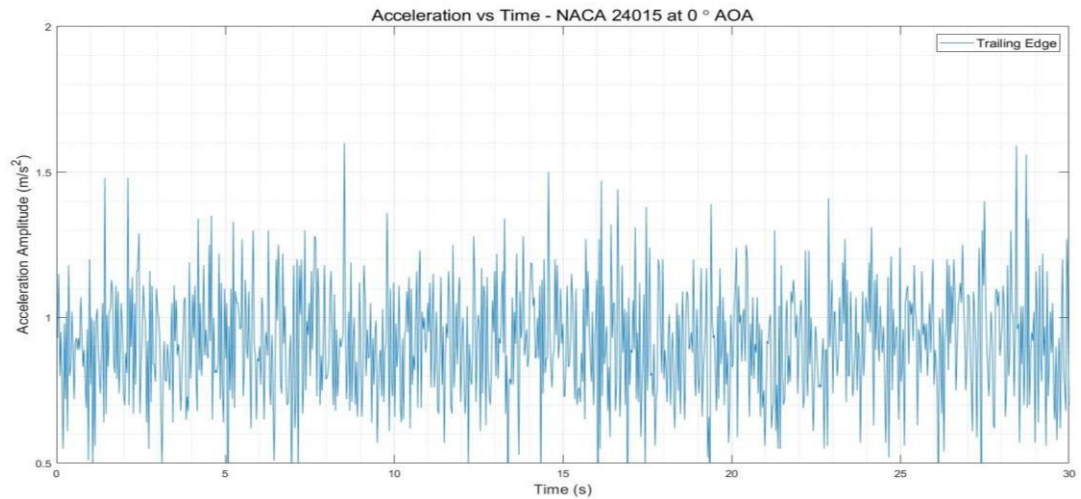


Figure 4.57: NACA 24015- 150 AOA- ACCELERATION VS TIME AT 28.8 m/s VELOCITY

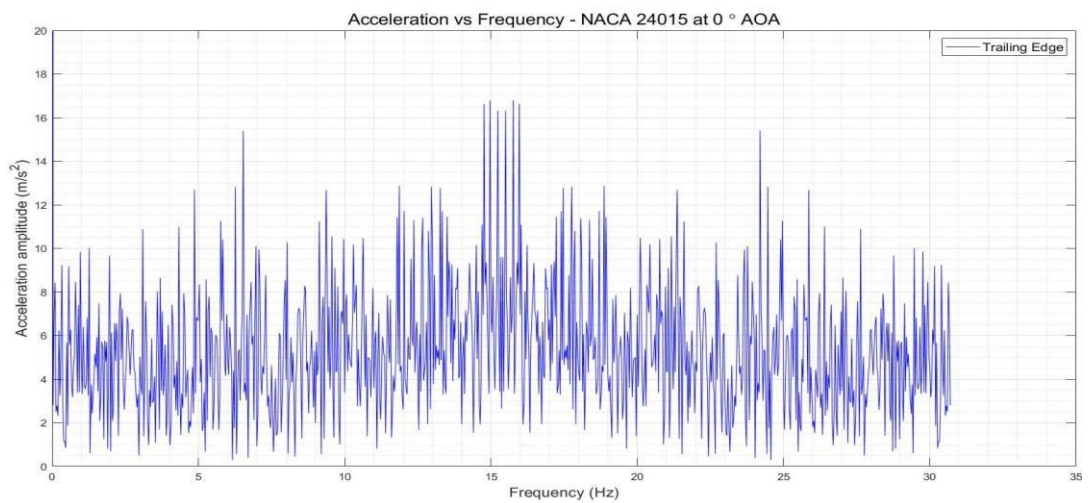


Figure 4.58: NACA 24015- 150 AOA- ACCELERATION VS FREQUENCY AT 28.8 m/s VELOCITY

ITERATION 30

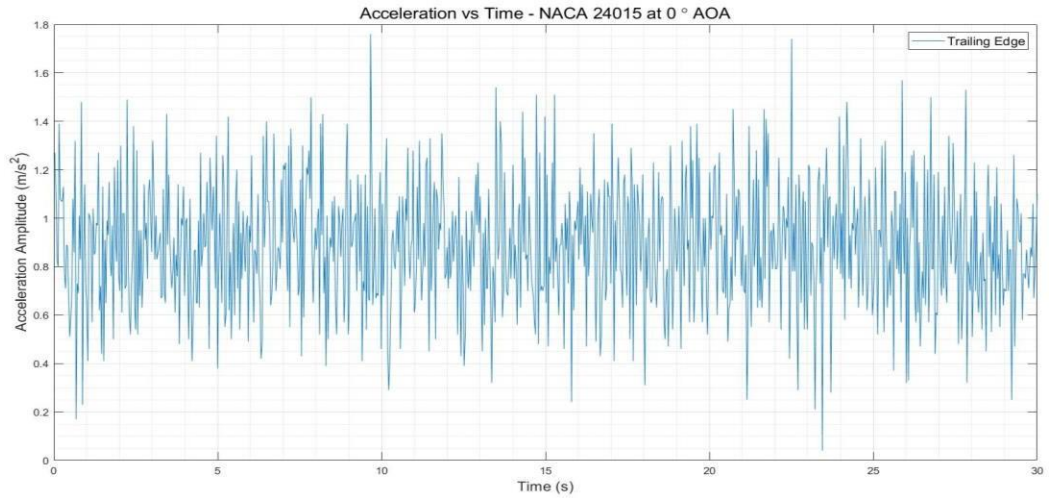


Figure 4.59: NACA 24015- 150 AOA- ACCELERATION VS TIME AT 32.7 m/s VELOCITY

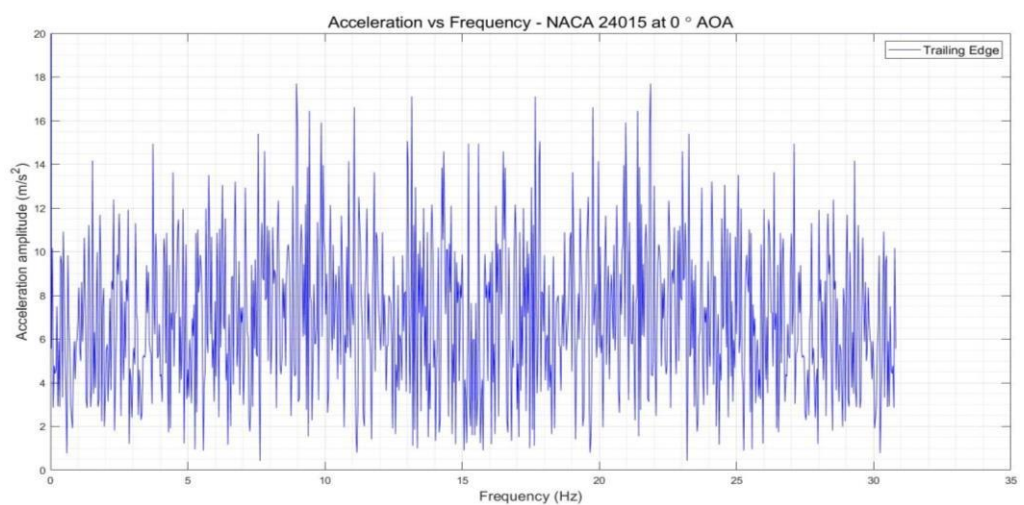


Figure 4.60: NACA 24015- 150 AOA- ACCELERATION VS FREQUENCY AT 32.7 m/s VELOCITY

Chapter 5

5 Conclusion and Future Scope

Based on the air inlet velocity at which flutter is induced and the intensity of flutter at specific air speeds, it can be concluded from the above displayed graphs that the flutter is induced at early airspeeds when the location of maximum camber is closer to the flexural axis which is at forty percent of the wing chord or to the aerodynamic center of the wing which is closer to the twenty five percentage of the chord length, the flutter seems to induce at lower air velocities and also if the closeness of the crests are observed in the graphs, it can be clearly understood that the flutter is more rigorous in the same case. If the graphs of 31015 airfoil are observed, where the flutter is not very intense at lower air velocities even at higher angle of attacks but if the plots of other airfoil are observed, it can be observed that the early most flutter can be seen for 34015 airfoil and even the intensity of the vibrations are also very high for the same wing and the only difference between these wings is the location of maximum camber. Hence from the above experiment and results, it can be understood that the location of maximum camber influences the flutter characteristics based on the location of the flexural axis.

Chapter 6

References

- [1.] D. Hodges, G. Pierce, and M. Cutchins, Authorized licensed use limited to: Auckland University of Technology. Introduction to Structural Dynamics and Aeroelasticity, vol. 56, no. 3. 2003.
- [2.] R. H. Scanlan, F. Sisto, E. H. Dowell, H. C. Curtiss, and H. Saunders, A Modern Course in Aeroelasticity, vol. 103, no. 2. 2010.
- [3.] R. M. Bennett, “Test Cases for Flutter of the Benchmark Models Rectangular Wings on the Pitch and Plunge Apparatus,” 2002.
- [4.] C. De Marqui Junior, D. C. Rebolho, E. M. Belo, F. D. Marques, and R. H. Tsubaki, “Design of an experimental flutter mount system,” J. Brazilian Soc. Mech. Sci. Eng., vol. 29, no. 3, pp. 246–252, 2007.
- [5.] G. Dimitriadi and J. Li, “Bifurcation Behavior of Airfoil Undergoing Stall Flutter Oscillations in Low-Speed Wind Tunnel,” AIAA J., vol. 47, no. 11, pp. 2577–2596, 2009.
- [6.] Bernard Etkin. Turbulent Wind and Its Effect on Flight. Journal of Aircraft, 18(5):327_345, 1981. doi:10.2514/3.57498.
- [7.] Liu, J., and Chan, H., “Limit Cycle Oscillations of Wing Section with Tip Mass,” Nonlinear Dynamics, Vol. 23, No. 3, 2000, pp. 259–270. doi:10.1023/A:1008361430662
- [8.] Gomez, J. C., and Garcia, E., “Morphing Unmanned Aerial Vehicles,” Smart Materials and Structures, Vol. 20, No. 10, 2011, Paper 103001. doi:10.1088/0964-1726/20/10/103001

[9.] Xu, J., and Ma, X. P., “Effects of Parameters on Flutter of Wing with an External Store,” Advanced Materials Research, Vol. 853, 2014, pp. 453–459, <https://www.scientific.net/AMR.853.453>.

[10.] Livne, E, “Aircraft Active Flutter Suppression: State of the Art and Technology Maturation Needs”, Journal of Aircraft, Vol. 55, No. 1, Jan.-Feb. 2018, pp. 410-452, doi: 10.2514/1.C034442.

[11.] Theodorsen, Th.: General Theory of Aerodynamic Instability and the Mechanism of Flutter. NACA Rept.496 (1934)

[12.] L. Marchetti, A. De Gaspari, L. Riccobene, F. Toffol, F. Fonte, S. Ricci and P. Mantegazza, Active Flutter Suppression Analysis and Wind Tunnel Studies of an Uncertain Commercial Transport Configuration,(2022)
doi: 10.2514/6.2020-1677

[13.] Y. D. DWIVEDI, Experimental Flow Field Investigation of the Bio-Inspired Corrugated Wing for MAV Applications,(2020)
doi: 10.13111/2066-8201.2021.13.2.5

[14.] Andreea KOREANSCHI, Mehdi ben HENIA, Olivier GUILLEMETTE, Flutter Analysis of a Morphing Wing Technology Demonstrator: Numerical Simulation and WindTunnel Testing(2016).
DOI: 10.13111/2066-8201.2016.8.1.10

[15.] Muhammad Ihtisham Babar, Experimental Flutter analysis of the Wing in Pitch and Plunge Mode 2019.

[16.] Muhammad Ihtisham Babar, DESIGN OF THE EXPERIMENTAL FLUTTER MECHANISM 2020.

[17.] Alessandro De Gaspari,Luca Riccobene, and Sergio Ricci, Design, Manufacturing and Wind Tunnel Validation of a Morphing Compliant Wing 2018.

[18.] Mehrdad Moradi and Morteza H. Sadeghi, Experimental and Theoretical Flutter Investigation for a Range of Wing Wind-Tunnel Models, DOI: 10.2514/1.C034311

[19.] Ivo Miguel Delgado Rocha, Experimental and Numerical Aeroelastic Study of Wings, 2019

[20.] Introduction to Structural Dynamics and Aero elasticity

[21.] Mechanical Vibrations, Singiresu S. Rao

[22.] A Modern Course in Aeroelasticity, Earl H. Dowell

CHAPTER 7

Appendix

1. The code:

Here is the code that is used to detect the acceleration data variations that occurred in the test section of the wind tunnel. This code is executed in **arduino 1.8.19 software**

```
#include <Wire.h>

// Wire library - used for I2C communication

int ADXL345_a = 0x53;
// The ADXL345 sensor I2C address
// SDO-> Vcc
// SDO-> GND

float Xa_out, Ya_out, Za_out;
// Outputs from Acce A

void setup()
{
    Serial.begin(9600);
    // Initiate serial communication for printing the results on the Serial monitor
    Wire.begin();
    // Initiate the Wire library
    // Set ADXL345 in measuring mode

    Wire.beginTransmission(ADXL345_a);
    // Start communicating with the device

    Wire.write(0x2D);
    // Access/ talk to POWER_CTL Register - 0x2D
    // Enable measurement

    Wire.write(8);
```

```

        // (8dec -> 0000 1000 binary) Bit D3 High for measuring enable
Wire.endTransmission();
delay(10);
}

void loop()
{
    // === Read accelerometer data from a === //
Wire.beginTransmission(ADXL345_a);
Wire.write(0x32);
    // Start with register 0x32 (ACCEL_XOUT_H)
Wire.endTransmission(false);
Wire.requestFrom(ADXL345_a, 6, true);
    // Read 6 registers total, each axis value is stored in 2 registers
Xa_out = ( Wire.read()| Wire.read() << 8);
    // X-axis value
Xa_out = Xa_out/256;
    //For a range of +-2g, we need to divide the raw values by 256, according to the
datasheet
Ya_out = ( Wire.read()| Wire.read() << 8);
    // Y-axis value
Ya_out = Ya_out/256;
Za_out = ( Wire.read()| Wire.read() << 8);
    // Z-axis value
Za_out = Za_out/256;

Serial.print("Xa= ");
Serial.print(Xa_out);
Serial.print(" Ya= ");
Serial.print(Ya_out);
Serial.print(" Za= ");
Serial.println(Za_out);

}

```

Here is the brief on the **MATLAB code** we used in this experimental process of obtaining different plots.

```
clc
clear
close all

%% READING ACCELEROMETER DATA and defining Variables
% LEADING EDGE %

data = xlsread('LE_500rpm.csv');
    % Importing accelerometer data

LE_time = data(:,1);
    % Assigning variables - time

LE_X_acc = data(:,2)
    % Assigning variables - X acceleration

LE_Y_acc = data(:,3);
    % Assigning variables - Y acceleration

LE_Z_acc = data(:,4);
    % Assigning variables - Z acceleration

%% FFT %%
N = numel(LE_time);
    % Number of time steps

Ts = abs(diff(LE_time(1:2)));
    % time interval per time step which is sampling time period

fs = 1/Ts;
    % Converting sampling time period to sampling frequency

f_axis = [0:N-1]*fs/N;
    % fs returns number of interval not frequency value, so here we convert
    % fs to frequency value using DFT(Discrete Fourier Transform) relations

A_freq_LE = fft(LE_Z_acc);
    % Converting acceleration values from time domain to frequency domain
    % using fast fourier transform

figure(1)
hold on
```

```

% hold on is used to plot multiple curves in same graph
plot(f_axis,abs(A_freq_TE),'-r','LineWidth',0.5)

% plotting frequency vs acceleration graph for LE

grid on
grid minor

% TRAILING EDGE %

data = xlsread('TE_500rpm.csv');

% Importing accelerometer data

TE_time = data(:,1);

% Assigning variables - time

TE_X_acc = data(:,2);

% Assigning variables - X acceleration

TE_Y_acc = data(:,3);

% Assigning variables - Y acceleration

TE_Z_acc = data(:,4);

% Assigning variables - Z acceleration

%% FFT %%

N = numel(TE_time);
Ts = abs(diff(TE_time(1:2)));
% Number of time steps
% time interval per time step which is sampling time period
fs = 1/Ts;
% Converting sampling time period to sampling frequency

f_axis = [0:N-1]*fs/N;
A_freq_TE = fft(TE_Z_acc);
% fs returns number of interval not frequency value, so here we
convert fs to frequency value using DFT(Discrete Fourier Transform) relations
% Converting acceleration values from time domain to frequency
domain using fast fourier transform
figure(1)
plot(f_axis,abs(A_freq_TE),'-b','LineWidth',0.5)

% plotting frequency vs acceleration graph for TE

grid on
grid minor

```

```

ylabel('Acceleration amplitude (m/s^2)','FontSize',14,'FontWeight','normal')

% Giving axis labels

xlabel('Frequency (Hz)','FontSize',14,'FontWeight','normal')

% Giving axis labels

ylim([0 20])

% Giving limit values for Y axis

legend ('Leading Edge','Trailing Edge','FontSize',12,'FontWeight','normal')

% Assigning legend to plot for LE and TE curves

title('Acceleration vs Frequency - NACA 24015 at 0 \circ AOA','FontSize',16,'FontWeight','normal')

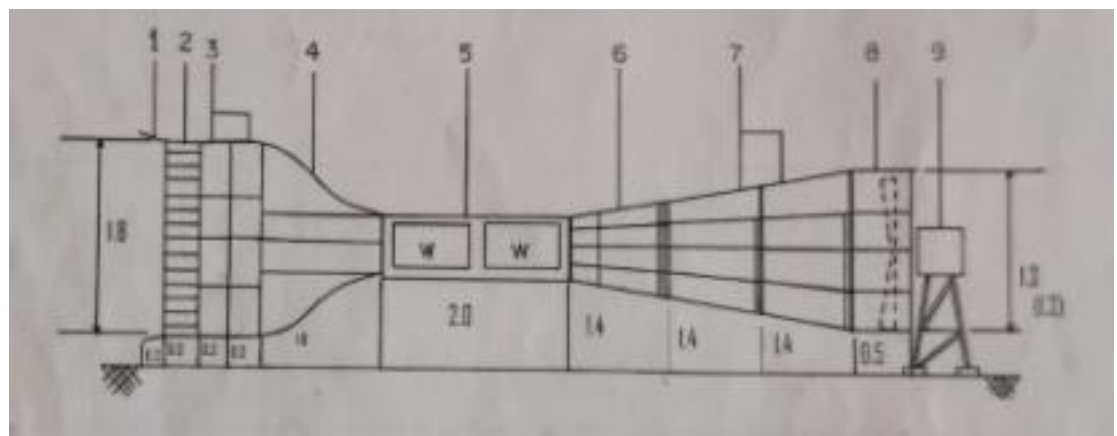
% Giving title to graph

```

2. The Facility:

The line sketch of the facility is given in the below figure with the main parts of the tunnel numbered from 1 to 9.

fig : Schematic diagram of wind tunnel.



PARTS :

1. Bell mouthed section
2. Honey comb
3. Settling chamber and screen sections
4. Contraction cone
5. Test section
6. Transition (square to circular)
7. Diffuser
8. Fan duct
9. Motor and stand

Experimental flutter analysis on an aircraft wing

ORIGINALITY REPORT

18% SIMILARITY INDEX	11% INTERNET SOURCES	9% PUBLICATIONS	% STUDENT PAPERS
--------------------------------	--------------------------------	---------------------------	----------------------------

PRIMARY SOURCES

- | | | |
|----------|--|-----------|
| 1 | stackoverflow.com
Internet Source | 3% |
| 2 | Khalid A. Alsaif, Mosaad A. Foda, Hachimi Fellouah. "Analytical and Experimental Aeroelastic Wing Flutter Analysis and Suppression", International Journal of Structural Stability and Dynamics, 2015
Publication | 2% |
| 3 | Muhammad Ihtisham Babar, Ali Javed, Farrukh Mazhar. "Design of the Experimental Flutter Mechanism", 2020 17th International Bhurban Conference on Applied Sciences and Technology (IBCAST), 2020
Publication | 2% |
| 4 | www.nitmanipur.ac.in
Internet Source | 2% |
| 5 | www.coursehero.com
Internet Source | 2% |
| 6 | Muhammad Ihtisham Babar, Ali Javed, Farrukh Mazhar, Rana Fahad Latif. | 1% |